
Bachelor's Degree in Engineering for Industrial Technologies

BACHELOR'S THESIS

# Optimal Energy Management of a Microgrid Considering Non-Linear Losses in the Lithium-Ion Battery

Author: María del Carmen García Pardo

Director: Javier García González

Madrid

Declaro, bajo mi responsabilidad, que el Proyecto presentado con el título

*Optimal Energy Management of a Microgrid Considering Non-Linear Losses in the Lithium-Ion Battery*

en la ETS de Ingeniería - ICAI de la Universidad Pontificia Comillas en el

curso académico 2023/24 es de mi autoría, original e inédito y

no ha sido presentado con anterioridad a otros efectos.

El Proyecto no es plagio de otro, ni total ni parcialmente y la información que ha sido

tomada de otros documentos está debidamente referenciada.

Fdo.: María del Carmen García Pardo Fecha: 27/ 05/ 2024

Autorizada la entrega del proyecto

EL DIRECTOR DEL PROYECTO

Fdo.: Javier García González Fecha: 27/ 05/ 2024


Bachelor's Degree in Engineering for Industrial Technologies

BACHELOR'S THESIS

# Optimal Energy Management of a Microgrid Considering Non-Linear Losses in the Lithium-Ion Battery

Author: María del Carmen García Pardo

Director: Javier García González

Madrid

# Acknowledgements

*To my family, without whom this wouldn’t have been possible.*

*To my director, Javier, for all the shared knowledge and guidance.*

# GESTIÓN ÓPTIMA DE ENERGÍA DE UNA MICRORRED CONSIDERANDO PÉRDIDAS NO-LINEALES EN LA BATERÍA DE ION-LITIO

**Autor: García Pardo, María del Carmen.**
Director: García González, Javier.
Entidad Colaboradora: ICAI – Universidad Pontificia Comillas

## RESUMEN DEL PROYECTO

Los sistemas de gestión de energía en microrredes eléctricas a menudo simplifican en exceso el modelado de la batería de ion-litio al considerar las pérdidas de potencia como lineales, lo cual puede llevar a una operación subóptima implicando costes de operación más elevados. Este proyecto tiene como objetivo incorporar una representación más realista del comportamiento de la batería desarrollando y resolviendo un modelo de optimización considerando pérdidas no lineales en la batería de ion-litio (*NLL*). Los resultados obtenidos al evaluar el rendimiento computacional de las combinaciones modelo-solver muestran que la combinación con mejor rendimiento supone resolver el modelo *NLL* usando DICOPT. También se ha concluido que usar un modelo con pérdidas lineales puede llevar a subestimar la verdadera eficiencia media de la batería de ion-litio, implicando costes de operación más elevados. Además, este proyecto muestra las ventajas de optimizar usando un horizonte móvil.

**Palabras clave**: Sistema de gestión de energía, microrred, pérdidas no-lineales, optimización, horizonte móvil

### 1. Introducción

Las microrredes están adquiriendo una importancia creciente debido a la necesidad de llevar a cabo una transición hacia soluciones energéticas más limpias, satisfacer la demanda energética creciente a nivel mundial, proveer acceso a electricidad en lugares remotos y aumentar la seguridad del suministro eléctrico. Los sistemas de gestión de energía son esenciales para el correcto funcionamiento de las microrredes. Sin embargo, el modelado de la batería en los modelos de optimización a menudo es simplificado en exceso, lo cual puede llevar a una operación subóptima de una microrred, implicando costes de operación más elevados.

### 2. Definición del proyecto

El objetivo de este proyecto es desarrollar y resolver un modelo de optimización para gestionar una microrred residencial aislada que consiste en una carga, un panel solar, un generador diésel, y una batería de ion-litio con pérdidas no-lineales durante la carga y la descarga. Los resultados obtenidos serán analizados para determinar el impacto de incorporar una representación más realista del comportamiento de una batería en el modelo de optimización del funcionamiento de una microrred.

## 3. Modelos de optimización

Dos modelos de optimización deterministas para la gestión de energía en una microrred han sido desarrollados y programados usando GAMS. Estos modelos se diferencian en las ecuaciones usadas para calcular las pérdidas de potencia durante la carga o descarga de la batería de ion-litio. En el modelo *LL*, se usan ecuaciones lineales para calcular las pérdidas de potencia en la batería de ion-litio mientras que en el modelo NLL se usan las ecuaciones no lineales derivadas en [1]. En estas ecuaciones las pérdidas no lineales son modeladas como funciones bivariantes de la potencia de carga/descarga y del estado de carga de la batería.

Además, se utilizarán dos enfoques de trabajo para implementar los modelos de optimización. El primero es un *enfoque de optimización de horizonte completo*, donde el modelo de optimización se resuelve una única vez para todo el horizonte temporal. El segundo es un *enfoque de optimización de horizonte móvil*, que supone resolver el problema de optimización de forma iterativa definiendo un horizonte de programación (SH), un horizonte de predicción (SH) y un horizonte de control (CH) y siguiendo la dinámica mostrada en la Figura 1.

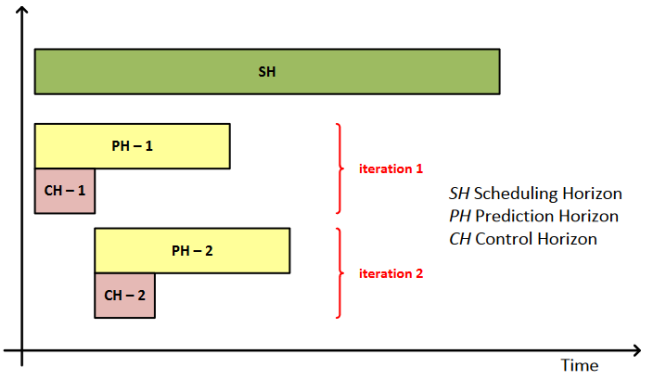


*Figura 1: Horizontes temporales en el enfoque de optimización de horizonte móvil (Fuente: [2])*

## 4. Resultados

### 4.1. Análisis Comparativo de Modelos de Optimización y Solvers

Los modelos estudiados incluyen *LL*, *NLL* y *ZZI-J1*. Este último, presentado en [1], utiliza aproximaciones lineales por tramos de las ecuaciones de pérdidas de potencia no lineales implementadas mediante una formulación entera de zig-zag. Para determinar el rendimiento de las combinaciones modelo-solver, estas han sido probadas usando un conjunto de datos de 168 horas obtenido en [3] y aplicando un *enfoque de optimización de horizonte completo*. Los resultados se muestran en la Tabla 1.

| ***Modelo*** | ***Solver Principal*** | ***Relaxed*** | ***Sub-solver MIP*** | ***Sub-solver NLP*** | ***Obj. [€]*** | ***Tiempo [s]*** | ***Rel. Gap*** |
|---|---|---|---|---|---|---|---|
| LL | GUROBI | - | - | - | 5.4197 | 5.69 | 0.32% |

| | | | | | | | |
|---|---|---|---|---|---|---|---|
| NLL | DICOPT | 1 | GUROBI | CONOPT | 7.0354 | 3613.14 | - |
| NLL | DICOPT | 1 | GUROBI | IPOPT | - | - | - |
| NLL | DICOPT | 1 | GUROBI | MINOS | 6.9869 | 11.11 | - |
| NLL | DICOPT | 1 | GUROBI | SNOPT | 6.8991 | 6.09 | - |
| NLL | DICOPT | 0 | GUROBI | CONOPT | 4.7509 | 35.47 | - |
| NLL | DICOPT | 0 | GUROBI | IPOPT | 4.7509 | 3631.53 | - |
| NLL | DICOPT | 0 | GUROBI | MINOS | 4.7509 | 23.97 | - |
| NLL | DICOPT | 0 | GUROBI | SNOPT | 4.7510 | 133.20 | - |
| NLL | BARON | - | Default | Default | 4.7421 | 3603.14 | 1.72% |
| NLL | BARON | - | Default | MINOS | 4.7436 | 3602.42 | 1.74% |
| NLL | BARON | - | Default | SNOPT | 4.7426 | 3602.50 | 1.73% |
| NLL | BARON | - | Default | IPOPT | 4.7459 | 3602.27 | 1.79% |
| ZZI-J1 | GUROBI | - | - | - | 4.7526 | 139.53 | 0.38% |

*Tabla 1: Resumen del rendimiento computacional de las combinaciones modelo-solver*

El modelo con mejor rendimiento computacional considerando tanto el tiempo de ejecución como el valor de la función objetivo (coste de operación semanal) ha sido *NLL*-DICOPT fijando las variables binarias en el NLP inicial usando los resultados de *LL*-GUROBI, específicamente con MINOS como sub-solver NLP. La Figura 2 ilustra cómo la energía es gestionada por esta combinación modelo-solver.

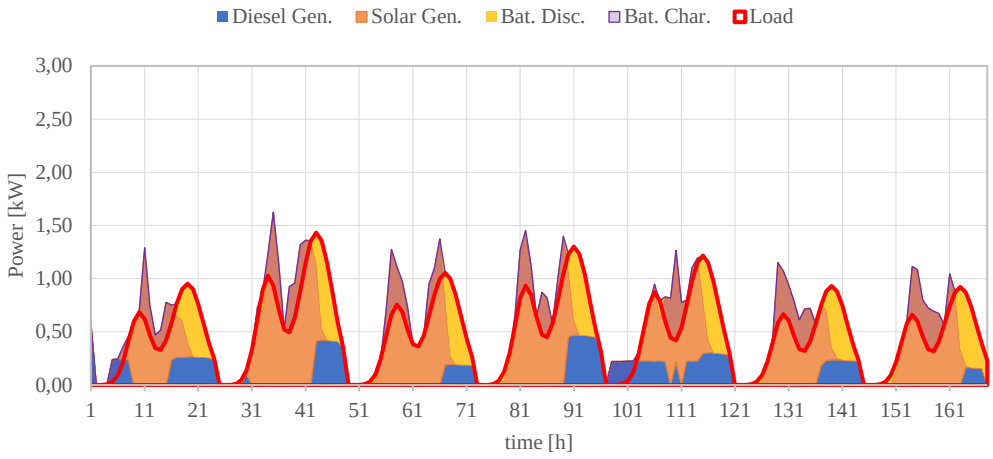


*Figura 2: Abastecimiento de la demanda (NLL, DICOPT, relaxed=0, GUROBI-MINOS, 168 horas)*

La Figura 2 muestra que el pico de carga de la batería ocurre durante el pico de generación solar y, por la tarde, la batería se descarga para ayudar a abastecer el pico de demanda. Normalmente, el generador diésel está encendido durante los picos de demanda por la tarde ya que el nivel de irradiación solar es bajo y la batería no es capaz de suministrar toda la potencia demandada por si sola. Sin embargo, en el día 5, la irradiación solar es más baja que el resto de los días, consecuentemente, el generador diésel suministra potencia prácticamente durante todo el día.

Al analizar la operación de los componentes de la microrred para diferentes combinaciones modelo-solver, se identificó que *ZZI-J1* tiene un valor de la función objetivo superior debido a que el panel solar suministra potencia a la microrred de forma menos uniforme que otros modelos, presentando picos muy pronunciados. Esto resulta en picos de carga de la batería notablemente más altos y por ende pérdidas de potencia mayores. Por lo tanto, es necesario un mayor uso de potencia diésel y se incurre en mayores costes de operación.

Aunque el modelo *LL*, en cuanto a tiempo de ejecución, supera a los demás modelos, en cuanto al valor de la función objetivo es menos efectivo. A través de la realización de un análisis de sensibilidad variando la eficiencia de la batería de ion-litio, se ha podido concluir que modelar las pérdidas como lineales puede llevar a subestimar la verdadera potencia media de la batería de ion-litio, implicando costes de operación más elevados. Esto resalta una clara desventaja de usar un modelo que considera pérdidas lineales.

### 4.2. Implementación del Enfoque de Optimización de Horizonte Móvil

Aunque *NLL*-BARON con la configuración por defecto de sub-solvers ha sido capaz de obtener el mejor valor de función objetivo, tuvo el tiempo de ejecución más largo. Para intentar resolver este inconveniente, se ha explorado la posible implementación del enfoque de horizonte móvil usando dos conjuntos de datos (uno correspondiente a una semana en verano y el otro a una semana en invierno). Los horizontes temporales usados se incluyen en la Tabla 2 y los resultados obtenidos se muestran en la Tabla 3.

| ***Horizonte temporal*** | ***Longitud de tiempo [h]*** |
|---|---|
| Horizonte de planificación (SH) | 168 |
| Horizonte de predicción (PH) | 24 |
| Horizonte de control (CH) | 8 |

*Tabla 2: Horizontes temporales*

| ***Set de datos*** | ***Enfoque de optimización*** | ***Obj. [€]*** | ***Tiempo [s]*** |
|---|---|---|---|
| Verano | Horizonte completo | 4.7421 | 3603.14 |
| Verano | Horizonte móvil | 4.7251 | 1524.06 |
| Invierno | Horizonte completo | 19.0309 | 765.69 |
| Invierno | Horizonte móvil | 19.0190 | 578.50 |

*Tabla 3: Resumen del rendimiento computacional de NNL-BARON*

Este enfoque de optimización mejora el rendimiento computacional de *NLL*-BARON, disminuyendo tanto el valor de la función objetivo como el tiempo de ejecución.

Además, esta implementación sirve como simulación de la operación real de una microrred. La principal diferencia en cuanto a la gestión de la energía es que al usar un enfoque de horizonte móvil, el modelo aprovecha más la irradiación solar disponible, como se muestra en la Figura 3.

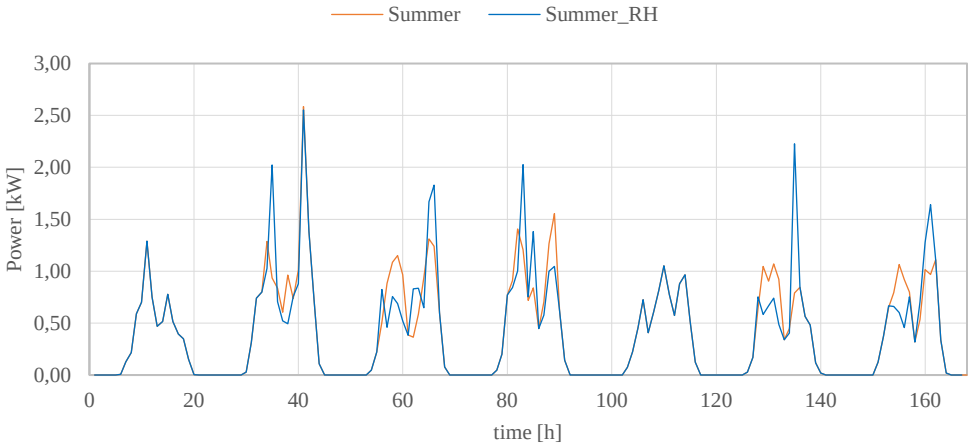


*Figura 3: Generación Solar (NLL-BARON, 168 horas Verano)*

## 5. Conclusiones

Los resultados obtenidos muestran una clara ventaja al usar un modelo de optimización que considera pérdidas no-lineales en la batería de ion-litio. Las combinaciones modelo-solver con mejor rendimiento son *NLL*-DICOPT fijando las variables binarias en el NLP inicial y *NLL*-BARON con las configuraciones por defecto al implementarlo usando un horizonte móvil.

En general, este proyecto contribuye a aumentar la precisión y efectividad de la gestión de energía en microrredes, reduciendo costes de operación.

## 6. Referencias


[1] García-González, J., & Guerrero, S. (2024). Optimal management of a microgrid Li-Ion battery considering non-linear losses using the Integer Zig-Zag formulation. *23rd Power Systems Computation Conference.*

[2] Silvente, J., Kopanos, G. M., Dua, V., & Papageorgiou, L. G. (2018). A rolling horizon approach for optimal management of microgrids under stochastic uncertainty. *Chemical Engineering Research and Design, 131,* 293–317. https://doi.org/10.1016/j.cherd.2017.09.013

[3] François-Lavet, V., & Taralla, D. DeeR. (2016). Disponible online: http://deer.readthedocs.io

# OPTIMAL ENERGY MANAGEMENT OF A MICROGRID CONSIDERING NON-LINEAR LOSSES IN THE LITHIUM-ION BATTERY

**Author: García Pardo, María del Carmen.**
Supervisor: García González, Javier.
Collaborating Entity: ICAI – Universidad Pontificia Comillas

## ABSTRACT

Energy management systems in electrical microgrids often oversimplify the modeling of the lithium-ion battery by considering power losses as linear, which can lead to a suboptimal operation implying higher operation costs. This project is aimed at incorporating a more realistic representation of battery behavior by developing and solving an optimization model considering non-linear power losses in the Li-ion battery (*NLL*). The results obtained when evaluating the computational performance of model-solver combinations shows that the best-performing combination involved solving model *NLL* using DICOPT. It was also concluded that using a model with linear losses can lead to underestimating the actual average efficiency of the Li-ion battery implying higher operation costs. Moreover, this project shows the advantages of using a rolling horizon optimization approach.

**Keywords**: Energy management system, microgrid, non-linear losses, optimization, rolling horizon

### 1. Introduction

Microgrids are gaining an increasing significance due to the need to transition towards cleaner energy solutions, meet increasing energy demands worldwide, provide access to electricity in remote locations and increase power reliability. Energy management systems are essential to the correct functioning of microgrids. However, the modelling of the battery in optimization models is often oversimplified, which can lead to a suboptimal operation of a microgrid, implying higher operation costs.

### 2. Project Description

The objective of this project is to develop and solve an optimization model to manage an isolated residential microgrid which consists of a load, a solar panel, a diesel generator, and a lithium-ion battery with non-linear power losses when charging and discharging. Results obtained will be analyzed to determine the impact of incorporating a more realistic representation of battery behavior into a microgrid optimization model.

### 3. Optimization models

Two deterministic optimization models for the energy management of the microgrid have been developed and coded using GAMS. These models differ in the equations used to calculate the power losses when the Li-ion battery is charging or discharging. In model

*LL*, linear equations are used to calculate the power losses in the Li-ion battery whereas model *NLL* involves the use of non-linear equations derived in [1]. Through these equations, power losses are modeled as bivariate functions of the charging/discharging power and the state of charge of the battery.

Moreover, two frameworks will be used to implement the optimization models. The first one is a *whole horizon optimization approach*, where the optimization model is solved once for the whole time horizon. The second one is a *rolling horizon optimization approach*, which involves solving an optimization problem in an iterative manner by defining a scheduling horizon (SH), a prediction horizon (PH) and a control horizon (CH) and following the dynamic illustrated in Figure 1.

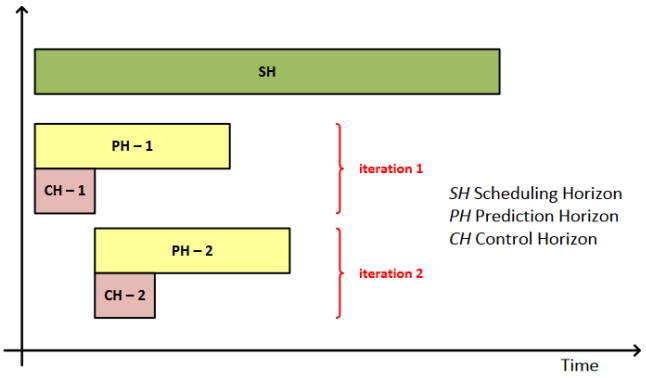


*Figure 1: Time horizons in rolling horizon framework (Source: [2])*

## 4. Results

### 4.1. Comparative Analysis of Optimization Models and Solvers

The models studied will include *LL*, *NLL* and *ZZI-J1*. The last model, which is presented in [1], uses piecewise linear approximations of the non-linear power losses equations implemented using an integer zig-zag formulation. To determine the performance of model-solver combinations, these have been tested using a 168-hour dataset obtained from [3] and applying a *whole horizon optimization approach*. The results are shown in Table 1.

| ***Model*** | ***Main Solver*** | ***Relaxed*** | ***MIP Sub-solver*** | ***NLP Sub-solver*** | ***Obj. [€]*** | ***Time [s]*** | ***Rel. Gap*** |
|---|---|---|---|---|---|---|---|
| LL | GUROBI | - | - | - | 5.4197 | 5.69 | 0.32% |
| NLL | DICOPT | 1 | GUROBI | CONOPT | 7.0354 | 3613.14 | - |
| NLL | DICOPT | 1 | GUROBI | IPOPT | - | - | - |
| NLL | DICOPT | 1 | GUROBI | MINOS | 6.9869 | 11.11 | - |
| NLL | DICOPT | 1 | GUROBI | SNOPT | 6.8991 | 6.09 | - |
| NLL | DICOPT | 0 | GUROBI | CONOPT | 4.7509 | 35.47 | - |
| NLL | DICOPT | 0 | GUROBI | IPOPT | 4.7509 | 3631.53 | - |
| NLL | DICOPT | 0 | GUROBI | MINOS | 4.7509 | 23.97 | - |
| NLL | DICOPT | 0 | GUROBI | SNOPT | 4.7510 | 133.20 | - |

| | | | | | | | |
|---|---|---|---|---|---|---|---|
| NLL | BARON | - | Default | Default | 4.7421 | 3603.14 | 1.72% |
| NLL | BARON | - | Default | MINOS | 4.7436 | 3602.42 | 1.74% |
| NLL | BARON | - | Default | SNOPT | 4.7426 | 3602.50 | 1.73% |
| NLL | BARON | - | Default | IPOPT | 4.7459 | 3602.27 | 1.79% |
| ZZI-J1 | GUROBI | - | - | - | 4.7526 | 139.53 | 0.38% |

*Table 1: Summary of computational performance of model-solver combinations*

The model which had the best computational performance considering both the execution time and the objective function value (weekly operation cost) was *NLL*-DICOPT fixing binary variables in the initial NLP using the results from *LL*-GUROBI, specifically when MINOS was used as the NLP sub-solver. Figure 2 illustrates how energy is managed by this model-solver combination.

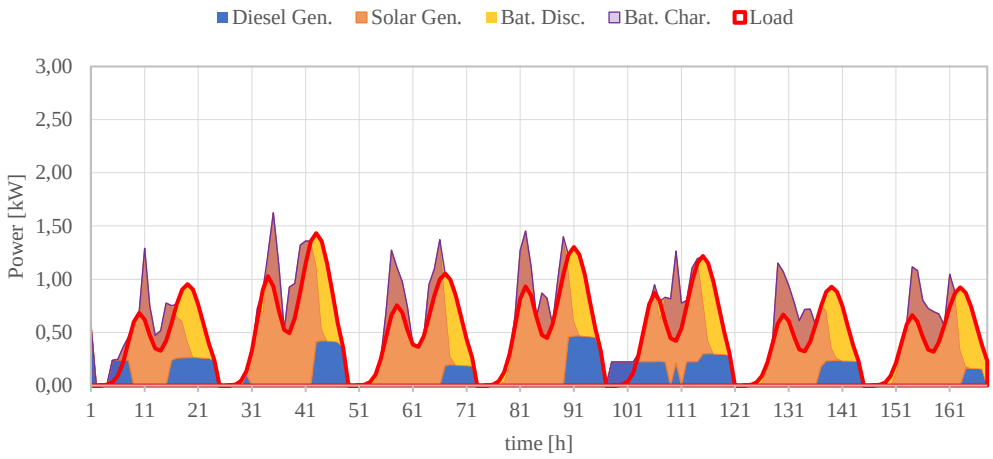


*Figure 2: Demand fulfillment (NLL, DICOPT, relaxed=0, GUROBI-MINOS, 168 hours)*

Figure 2 shows that the battery charging peak occurs during the solar generation peak and, during the evening, the battery discharges to help fulfill the demand peak. Usually, the diesel generator is on during demand peaks in the evening since the level of solar radiation is low and battery can't supply all the power demanded on its own. However, on day 5, the solar irradiation is lower than the rest of the days, consequently, the diesel generator supplies power practically throughout the whole day.

When analyzing the operation of the microgrid components for the different model-solver combinations, it was identified that *ZZI-J1* has a higher objective function value due to the solar panel supplying power to the microgrid in a less uniform way than other models, presenting very pronounced peaks. This resulted in notably higher battery charging peaks and hence increased power losses meaning more diesel power had to be used and greater operation costs were incurred.

Although model *LL*, in terms of execution time, outperforms all other models, in terms of objective function value it performed less effectively. Through carrying out a sensitivity analysis by varying the efficiency of the Li-ion battery, it was concluded

that modeling losses as linear can lead to underestimating the actual average efficiency of the Li-ion battery, implying higher operation costs. This highlights a clear drawback of using a model which considers linear losses.

### 4.2. Implementation of Rolling Horizon Optimization Framework

Although *NLL*-BARON with the default sub-solver configurations was able to obtain the best objective function value, it had the longest execution time. To address this, the implementation of a rolling horizon optimization approach was explored using two datasets (one corresponding to a week in summer and the other one to a week in winter). The time horizons used are included in Table 2 and the results are shown in Table 3.

| ***Time horizon*** | ***Time length [h]*** |
|---|---|
| Scheduling horizon | 168 |
| Prediction horizon | 24 |
| Control horizon | 8 |

*Table 2: Time horizons*

| ***Dataset*** | ***Optimization approach*** | ***Obj. [€]*** | ***Time [s]*** |
|---|---|---|---|
| Summer | Whole horizon | 4.7421 | 3603.14 |
| Summer | Rolling Horizon | 4.7251 | 1524.06 |
| Winter | Whole horizon | 19.0309 | 765.69 |
| Winter | Rolling Horizon | 19.0190 | 578.50 |

*Table 3: Summary of computational performance of NNL-BARON*

This optimization approach improved *NLL*-BARON's computational performance, decreasing both the objective function value and execution time.

Moreover, this implementation served as a simulation of the real-life operation of a microgrid. The main difference regarding energy management between both optimization approaches was that when using the rolling horizon framework, the model took more advantage solar irradiation available, as shown in Figure 3.

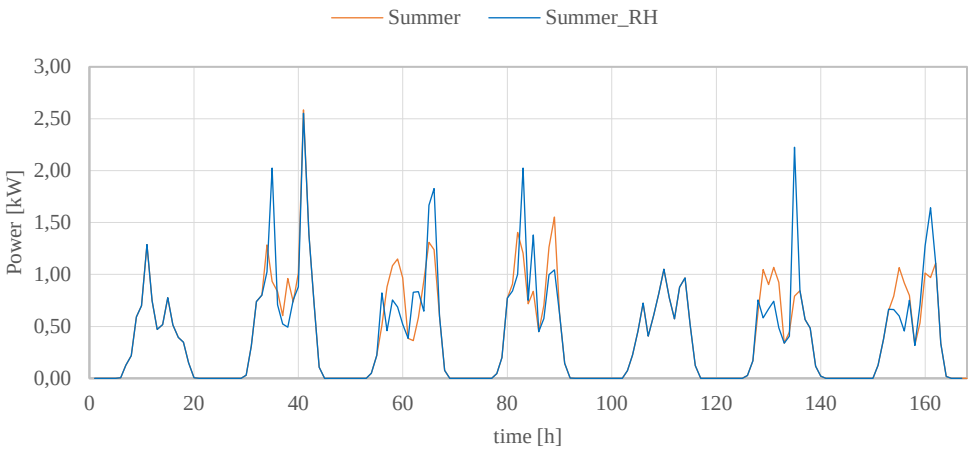


*Figure 3: Solar Generation (NLL-BARON, 168 hours Summer)*

## 5. Conclusions

The results obtained have shown a successful performance when using an optimization model which considers non-linear losses in the Li-ion battery. The best-performing models are *NLL*-DICOPT fixing binary variables in the initial NLP and *NLL*-BARON with the default sub-solver configurations when implemented using the rolling horizon framework.

Overall, this project contributes to the increase in accuracy and effectiveness of microgrid energy management, ultimately reducing operation costs.

## 6. References

[1] García-González, J., & Guerrero, S. (2024). Optimal management of a microgrid Li-Ion battery considering non-linear losses using the Integer Zig-Zag formulation. *23rd Power Systems Computation Conference.*

[2] Silvente, J., Kopanos, G. M., Dua, V., & Papageorgiou, L. G. (2018). A rolling horizon approach for optimal management of microgrids under stochastic uncertainty. *Chemical Engineering Research and Design, 131*, 293–317. https://doi.org/10.1016/j.cherd.2017.09.013

[3] François-Lavet, V., & Taralla, D. DeeR. (2016). Available online: http://deer.readthedocs.io

# *Contents*

# *List of Figures*

# *List of Tables*

# Chapter 1. INTRODUCTION

## *1.1 INTRODUCTION*

Energy is a key resource present in our everyday lives. Its applications range from residential usage to powering industries that drive the global economy, thereby ensuring society's well-being and progress. Population growth, technological advancements, and urbanization have significantly increased the demand for energy over the past decade [1] and, nowadays, it is essential for manufacturing, transportation, communications, medical equipment, climatization, and much more.

Although energy is a contributes notably to social and economic development, its decarbonization is an ongoing challenge. Over the past years, there has been a shift from fossil fuel power generation to reducing carbon emissions and addressing concerns regarding their limited supply. This is fostering a massive deployment of renewable energy sources (RES) within the electric power industry. Therefore, according to the International Energy Agency (IEA), renewables will become the largest source of global electricity generation by 2025. In fact, renewable energy is forecasted to grow almost 2400 GW between 2022 and 2027, which is equal to the entire installed power capacity of China in 2022. [2]

The presence of higher shares of RES in the generation mix will be led by two technologies: photovoltaic panels and wind turbines [2]. Both can be installed as distributed generation and combined with storage systems, such as batteries, to create micro-networks. These are known as microgrids, and they will be defined more specifically in section 1.2.

The use of microgrids not only enables transitioning towards cleaner energy but it is also a response to meet the increasing electricity demand worldwide. Demand for electricity is being driven by the electrification of sectors such as transport and heating as well as the growth of emerging and developing economies [3]. Over the next years, global electricity generation is expected to grow significantly and renewables will make up the majority of the

increase (Figure 1.1). Since microgrids are designed to incorporate various distributed energy resources, including solar panels and wind turbines, they will be beneficial for integrating and promoting the use of RES.

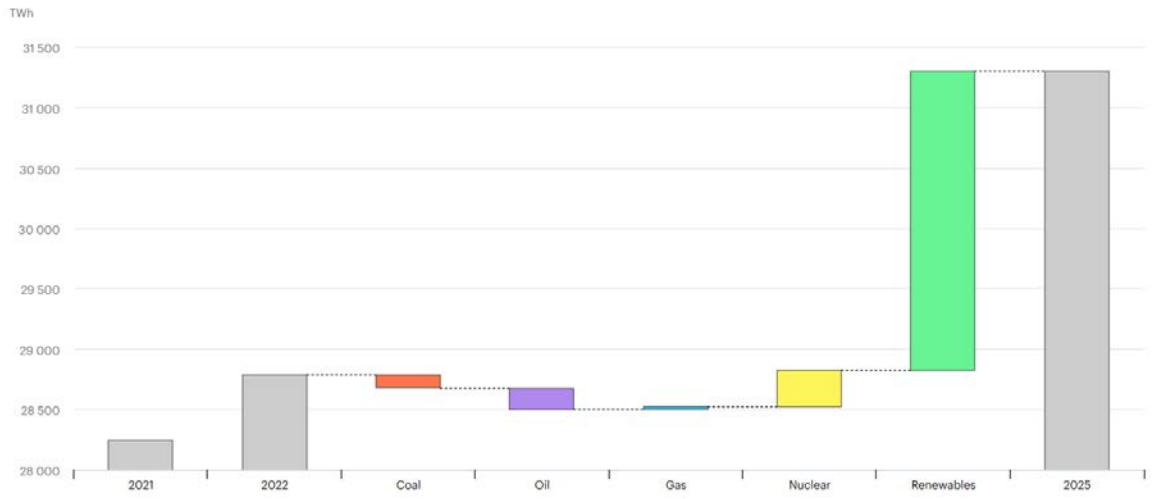


*Figure 1.1: Changes in global electricity generation by source, 2021-2025 (Source: [3])*

As global electricity demand grows, another challenge emerges: ensuring universal access to electricity. Microgrids can help address this problem by providing access to electricity in remote locations [4]. Extending the main grid to reach isolated communities can sometimes be too expensive or technically unviable so microgrids can serve as a practical alternative in these situations.

Moreover, microgrids can contribute to improving the reliability of power supply, which is especially relevant to protect critical systems from blackouts [5]. If electricity supply from the main grid to a country's critical infrastructure were to cease unexpectedly, being connected to a microgrid would enable systems to keep running by using energy from storage systems and distributed energy sources.

Overall, these factors will make the microgrid market keep growing in the coming years.

## *1.2 STATE OF THE ART*

A microgrid is a group of interconnected distributed energy resources, storage systems and loads that function as a single controllable entity [6]. Microgrids can either work grid-connected or islanded. In a grid-connected mode, microgrids operate as part of the larger utility grid, interacting and exchanging power with the external network. Alternatively, in islanded mode, the microgrid is disconnected from the main grid and relies solely on its internal resources to meet energy demand.

### 1.2.1 MICROGRID COMPONENTS

Microgrids can be composed of different elements, however, in the literature, the most common components are shown in Figure 1.2 and include the following:

**Loads**, such as households. Most loads have a variable power consumption which cannot be predicted with certainty.

**Renewable energy sources** (RES), such as photovoltaic panels and wind turbines. Using RES can be beneficial from both a financial and an environmental point of view [7]. Once the initial investment is made in the infrastructure, the ongoing operation and maintenance costs of renewable energy systems can be lower than traditional fossil fuel-based systems.

**Energy storage systems** (ESS), such as Li-ion batteries or a $H_2$ storages. RES are intermittent and uncertain, meaning that their supply will not remain constant throughout the day and cannot be perfectly forecasted. ESS typically consume or generate power depending on whether generation is greater than demand or vice versa. This helps minimize costs since, if at one point in the day power generated by RES is greater than the one demanded, it can be stored and used later when there is a power shortage. [8]

**Conventional generation sources**, such as a diesel group or a microturbine. In an islanded microgrid, RES and ESS might not be enough to satisfy the demand at certain times of the day so other energy sources must be included to avoid power shortages. [5]

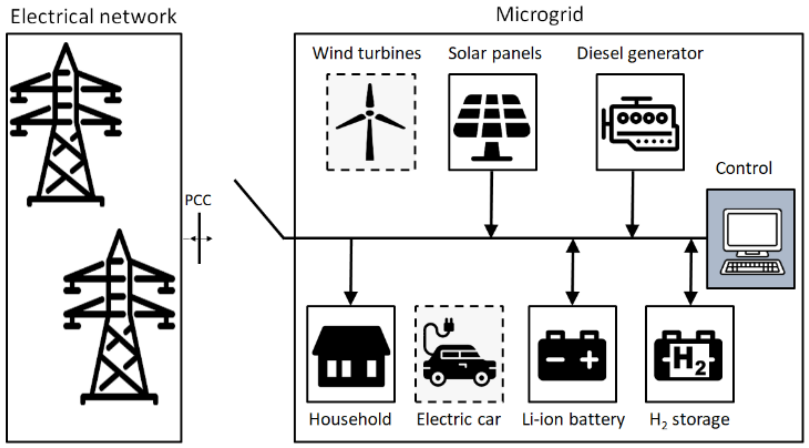


*Figure 1.2: Schematic representation of a possible microgrid setup (Source: [5])*

Electric vehicles are additional loads during the charging process, and in case the vehicle to grid (V2G) mode is available, they can act as generators providing electricity to the microgrid using the energy stored in their batteries.

### 1.2.2 MICROGRID ENERGY MANAGEMENT SYSTEMS

All the components in a microgrid must be controlled in such a way that certain operational constraints are met and profits or costs, either economic or environmental, are maximized or minimized. Coordinating a microgrid can be challenging; therefore, to optimize its operation, Energy Management Systems (EMS) are used. A microgrid EMS is a control and optimization system designed to efficiently manage energy generation, storage, and consumption within a microgrid. These systems are especially relevant given the intermittent and stochastic nature of the energy management problem resulting from both the use of RES and variable loads. EMS ensure an efficient, reliable, and economical operation of microgrids [9].

### *1.2.2.1 Optimization Techniques Used in Energy Management Systems*

Different optimization techniques have been proposed to solve the energy management problem in the literature. These can be classified into four groups: AI method-based EMS, Conventional method-based EMS, Metaheuristics method-based EMS, and Other method-based EMS. [1]

Figure 1.3 shows that mixed integer programming (MIP) is the most popular optimization technique for energy management of microgrids. This is due to the fact that it offers a rigorous and versatile approach to address the complex decision-making processes involved in EMS. MIP is used to model problems that involve both continuous and integer variables using constraints and an objective function. This technique stands out for its performance and simplicity [1], making it highly suitable for optimizing energy management in microgrids.

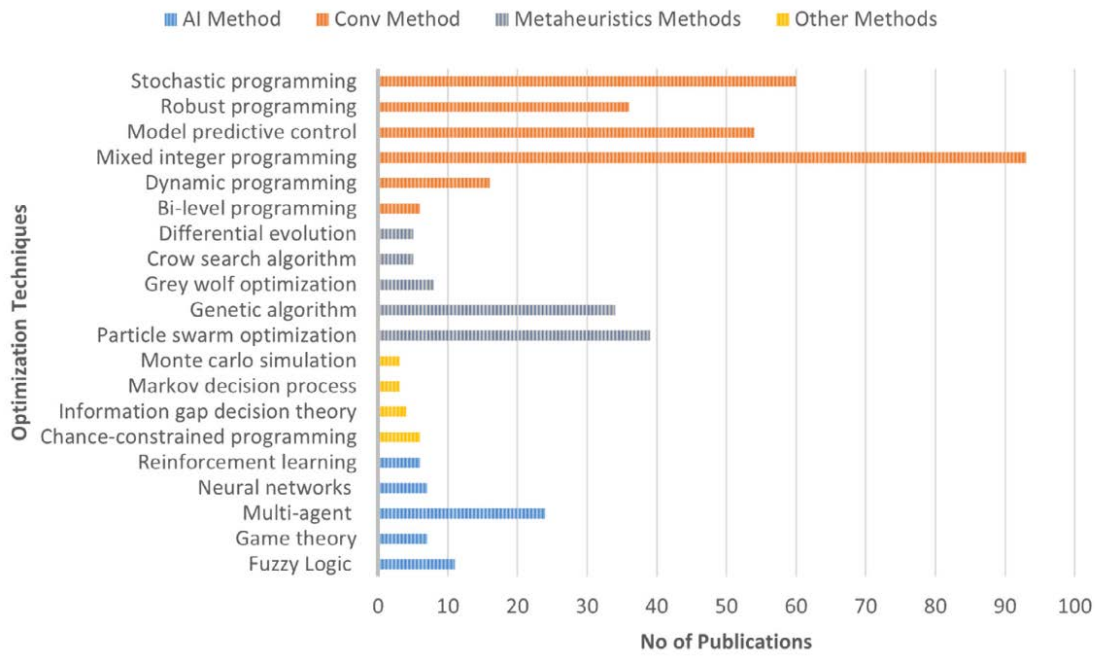


*Figure 1.3: Analysis of different optimization techniques based on the number of publications during 2010–2020 (Source: [1])*

Energy management schemes in the context of microgrids can pursue one or multiple objectives, being the following the most common [1]:

- **Forecasting**: Predicting future load or generation profiles.
- **Economic/environmental dispatch**: Increasing environmental/economic benefits by improving the utilization of the microgrid's elements.
- **Unit commitment**: Coordinating electricity generators to fulfil demand minimizing costs and maximizing revenue if fossil fuel-based generators that require to be started-up or shut-down are being used together with RES.
- **Demand management**: Scheduling load effectively to increase financial benefit.

Depending on the optimization technique used, pursuing certain objectives is more usual in the literature. This analysis is shown graphically in Figure 1.4.

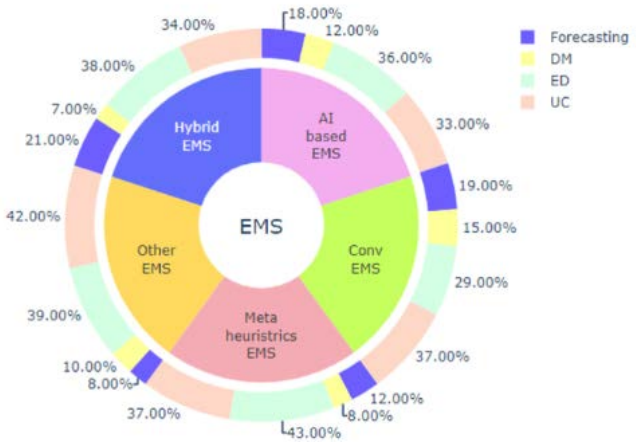


*Figure 1.4: Distribution of the objective of the EMS with respect to the type of optimization techniques (Source: [1])*

From the chart presented, it can be deduced that the majority of the objectives are pursued in a similar proportion amongst the different optimization techniques, being unit commitment and environmental/economic dispatch the objectives which are addressed most by all of the techniques.

According to [1], the most cited paper within the field of AI method-based optimization is [10], which aims to minimize the operation cost and the environmental impact of a microgrid. This is done by formulating an energy management problem and solving it using linear-programming-based multi-objective optimization together with artificial intelligence techniques. This paper pursues three of the objectives mentioned above: forecasting, environmental/economic dispatch, and unit commitment. A fuzzy logic expert system is used for the scheduling of the battery, considering linear losses.

[11] was identified as one of the most cited papers within conventional method-based optimization by [1]. The study focuses on component size optimization, optimal scheduling of shiftable appliances, and demand response planning. The decision variables included the capacity of RES (photovoltaic panels and wind turbines) and ESS (batteries, considering linear losses) and the operation times for dispatchable loads.

Within metaheuristics method-based techniques, [11] proposes an optimal probabilistic energy management of a typical microgrid using robust optimization and a point estimate method. Microgrid components include a microturbine, a diesel generator, a battery (considering linear losses), a photovoltaic panel and a wind turbine. This paper also seeks to compare deterministic and probabilistic management in different scenarios.

## *1.3 MOTIVATION*

Microgrid energy management systems are gaining an increasing significance given the need for sustainable energy solutions and efficient management of distributed energy resources.

Literature on microgrid EMS focuses on a diverse range of topics from optimal sizing to demand response. However, regarding the modelling of the battery in the microgrids, the consideration of non-linear losses has not been explored much. This implies that battery dynamics are often oversimplified, which can lead to a suboptimal operation of a microgrid, implying higher operation costs.

Therefore, this project will be aimed at incorporating a more realistic representation of battery behavior by developing an optimization model to manage a residential microgrid which consists of a load, a solar panel, a diesel generator, and a lithium-ion battery with non-linear power losses when charging and discharging. An islanded microgrid will be studied since the main focus of the EMS will be the modelling of the Li-ion battery. By studying the implications of considering non-linear losses, the project aspires to increase the accuracy and effectiveness of microgrid energy management, ultimately contributing to the advancement of sustainable and reliable energy infrastructures.

## *1.4 OBJECTIVES*

Main objectives:

- Formulate an optimization model for the energy management of a microgrid which consists of a solar panel, a diesel generator, and a lithium-ion battery with linear losses (model *LL*).
- Modify the previous formulation to account for non-linear losses when charging and discharging the lithium-ion battery (model *NLL*).
- Code and implement both optimization models.
- Compare the obtained results when considering linear versus non-linear losses in the lithium-ion battery.

Additional objectives:

- Analyze the impact of the optimization problem solver chosen on the computational performance and the energy management of the microgrid.
- Compare the obtained results when solving the optimization models developed in the project with other models proposed in the literature.
- Carry out a sensitivity analysis considering different Li-ion battery efficiencies.

- Formulate, code and integrate a rolling horizon optimization framework into both microgrid models.
- Analyze and compare results obtained when using a *rolling horizon optimization approach* versus a *whole horizon optimization approach*.

## *1.5 METHODOLOGY AND RESOURCES*

The methodology for this project will be the following:

- Definition of microgrid components: A review of existing literature regarding the components used in residential microgrids will be carried out in order to choose the characteristics of the components for this project's microgrid model. This will include the research and selection of solar panel generation profile data and load profile data.
- Formulation of the optimization models: Models will be formulated using mixed-integer programming due the advantages mentioned in a previous section and its extensive use in literature, meaning it provides a solid base on which to build and innovate. Furthermore, it is mostly used in unit commitment, which will be the main objective of the models developed.
- Coding of optimization models: In this phase, both models will be coded in the General Algebraic Modelling System (GAMS) [12].
- Research of GAMS solvers: Conduct a review of academic papers and GAMS manuals to identify potential GAMS solvers that could be used to solve the optimization problems.
- Validation of optimization models: To ensure the correct functioning of both models, various trials will be carried out with multiple datasets and solvers. Results will be analyzed to identify and address any potential issues.

- Case study analysis: The optimization models will be solved for a given case study and results obtained will be analyzed to compare model performance and energy management for different model and solver combinations.

To complete the project, the schedule shown in Table 1.1 has been followed.

| *Month* | *Tasks* |
|---|---|
| January | State of the art |
| February | Definition of microgrid components |
| | Formulation of optimization models |
| | Coding of optimization models |
| March | Validation of optimization models |
| | Research of GAMS solvers |
| April | Validation of optimization models |
| | Research of GAMS solvers |
| May | Case study analysis |
| | Report write-up |

*Table 1.1: Project Schedule*

# Chapter 2. MICROGRID COMPONENTS

This chapter provides a comprehensive overview of the components comprising the microgrid studied in the project: a load, a solar panel, a diesel generator, and a lithium-ion battery, as shown in Figure 2.1. Each component is described in detail, including its function, operational characteristics, and specifications.

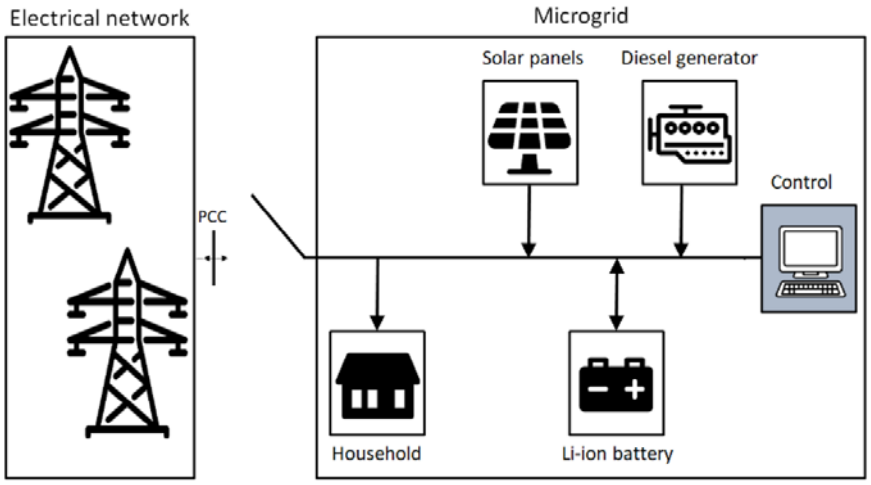


*Figure 2.1: Schematic representation of microgrid studied*

This project focuses on the operation phase of a microgrid and therefore, the optimal sizing of the microgrid is beyond its scope and initial investment costs for each component will not be evaluated. The characteristics of the microgrid components will be chosen based on those proposed in papers [5] and [13].

## 2.1 LOAD

The load for the microgrid studied will be a residential household with a power demand which is independent of the operation state of the other components connected to the microgrid. Household power consumption varies throughout the day and, therefore, it will

be modeled using an hourly time series obtained from [14]. The dataset chosen consists of three years of hourly data for the power demanded by a typical household with a daily average consumption of 18kWh.

Since the microgrid is not connected to the main grid, scenarios where power demanded in a given hour exceeds the total power microgrid components can supply during that period are possible. To penalize energy shortages when optimizing energy management, a cost of 1 € per kWh of non-supplied energy will be accounted for.

Throughout the model validation process, it was determined that this demand was too high for the characteristics of the microgrid studied given the ratio of non-served energy to supplied energy. Consequently, the demand was adjusted by applying a 30% decrease to the whole time series. Figure 2.2 shows the resulting demand profile for a time window of 168 hours.

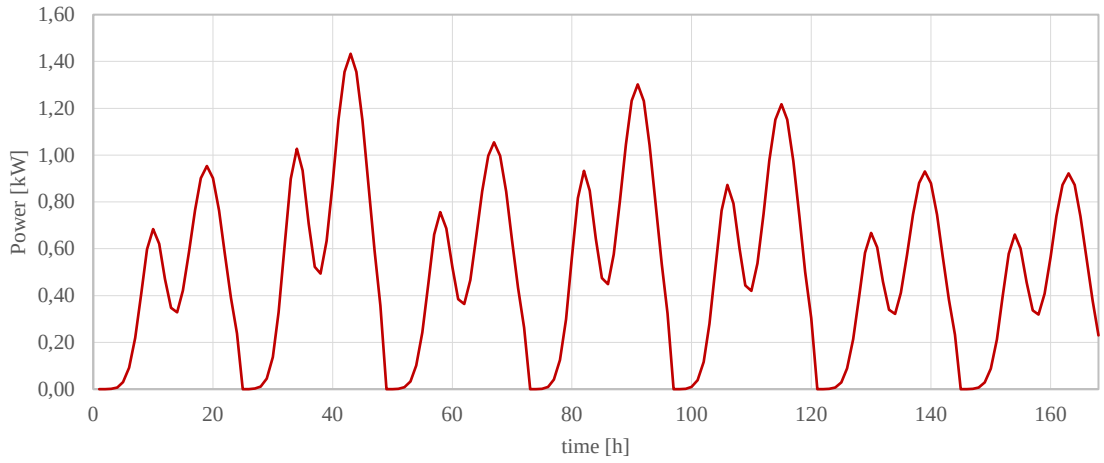


*Figure 2.2: Hourly load for a 168-hour period*

## 2.2 SOLAR PANEL

Solar panels are energy-generating components in the microgrid whose power output depends on the weather and the position of the sun relative to the solar panels. If not all of the power generated by the solar panel is required to fulfill power demand, it can be curtailed. This means that the net power supplied by the solar panel does depend on the operation of other components in the microgrid. It is assumed that this energy spillage does not imply an additional cost.

The solar panel in the microgrid studied will be modelled using a dataset from [14] which consists of an hourly time series of the power generated by photovoltaic panels for a residential customer located in Belgium. The complete dataset covers a period of three years. Figure 2.3 shows a 168-hour period taken from a summer month.

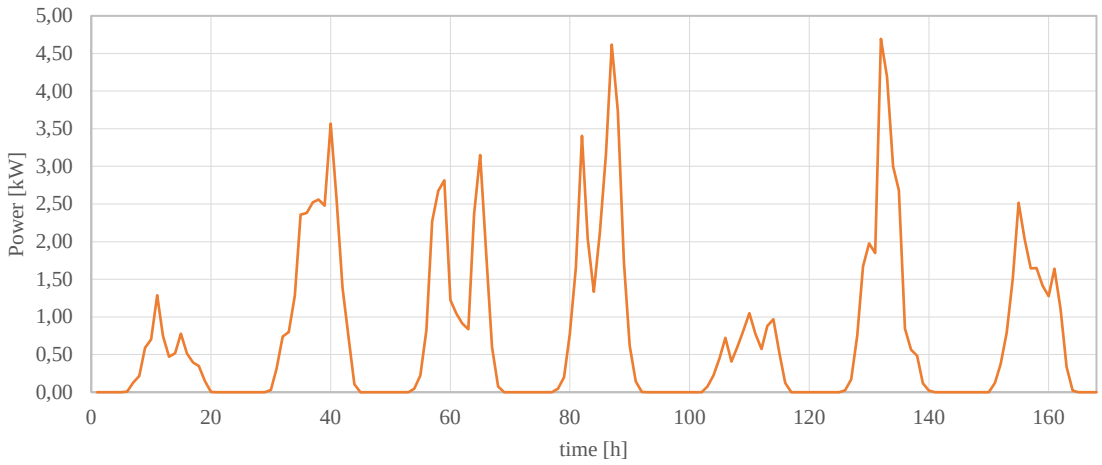


*Figure 2.3: Hourly available PV power for a 168-hour period in summer*

## 2.3 DIESEL GENERATOR

The integration of a diesel generator into the microgrid addresses the uncertainty associated with solar panel power supply. By providing a reliable backup, the diesel generator contributes to minimizing non-supplied energy during periods of low solar output when there is a lack of PV power production.

The operation of a diesel generator is managed by the control system can be modeled using two variables:

- $u_t^d$: A binary variable which indicates whether the diesel generator is on or off in period t.
- $p_t^d$: A positive continuous variable which indicates the power output of the diesel generator in period t. This value must be smaller than the diesel generator's maximum power output ($P_{max}^d$), whose value for the microgrid studied is indicated in Table 2.1.

Neglecting the cost associated with the diesel generator's start-up and shutdown, its total operating cost will be modeled as the sum of a fixed cost which is incurred if the generator is committed ($u_t^d$=1) and a variable cost modeled as a quadratic function of the diesel generator's power output [1]:

$$C_t\left(p_t^d, u_t^d\right) = a\ (p_t^d)^2 + b\ p_t^d + c\ u_t^d \tag{1}$$

In the microgrid studied, it will be assumed that the diesel generator is the only component for which a cost is incurred in its operation and parameters $a$, $b$ and $c$ will take the values shown in Table 2.1.

| *Parameter* | *Definition* | *Value* | *Units* |
|---|---|---|---|
| a | quadratic term of diesel generator cost-function | 0.31 | €/kW$^2$h |
| b | linear term of the diesel generator cost-function | 0.1080 | €/kWh |
| c | independent term of the diesel generator cost function when the generator is committed | 0.0157 | €/h |
| $P^d_{max}$ | maximum output power of diesel generator [kW] | 1.0 | kW |

*Table 2.1: Diesel generator parameters*

## 2.4 LITHIUM-ION BATTERY

The Li-ion battery is a component which can generate or consume power depending on whether it is charging or discharging. This feature provides flexibility to the microgrid given that, when managed optimally, the battery will charge during periods of high RES generation and discharge when RES generation is low, thereby reducing dependency on other more costly power sources such as the diesel generator.

Both the charging/discharging decision and the magnitude of the power consumed or generated are decision variables managed by the control system.

The Li-ion battery studied in this project is characterized by the parameters shown in Table 2.2.

| *Parameter* | *Definition* | *Value* | *Units* |
|---|---|---|---|
| $\eta^{b\ char}$ | charge efficiency of Li-ion battery | 0.9 | - |
| $\eta^{b\ disc}$ | discharge efficiency of Li-ion battery | 0.9 | - |
| $P^{b}_{max\ char}$ | maximum charge power of Li-ion battery | 2.9 | kW |
| $P^{b}_{max\ disc}$ | maximum discharge power of Li-ion battery | 2.9 | kW |
| $E^{b}_{0}$ | initial energy stored in Li-ion battery | 0.1 | kWh |
| $E^{b}_{min}$ | minimum energy storage of Li-ion battery | 0.01 | kWh |
| $E^{b}_{max}$ | maximum energy storage of Li-ion battery | 2.9 | kWh |
| $V_r$ | rated voltage of Li-ion battery | 51.2 | V |
| R | internal resistance of battery | 0.026464 | Ω |
| K | polarization coefficient | 0.0080625 | Ω |

*Table 2.2: Lithium-ion battery parameters*

### 2.4.1 POWER LOSSES IN LI-ION BATTERY

Power losses in the Li-ion battery will be modeled using two equations, one for the power losses when charging and the other for the power losses when discharging.

### *2.4.1.1 Equations for linear losses in Li-ion battery*

In this section, two linear equations for the power losses in the Li-ion battery will be derived: one for discharging losses and the other for charging losses. Figure 2.4 illustrates the variables involved in these equations.

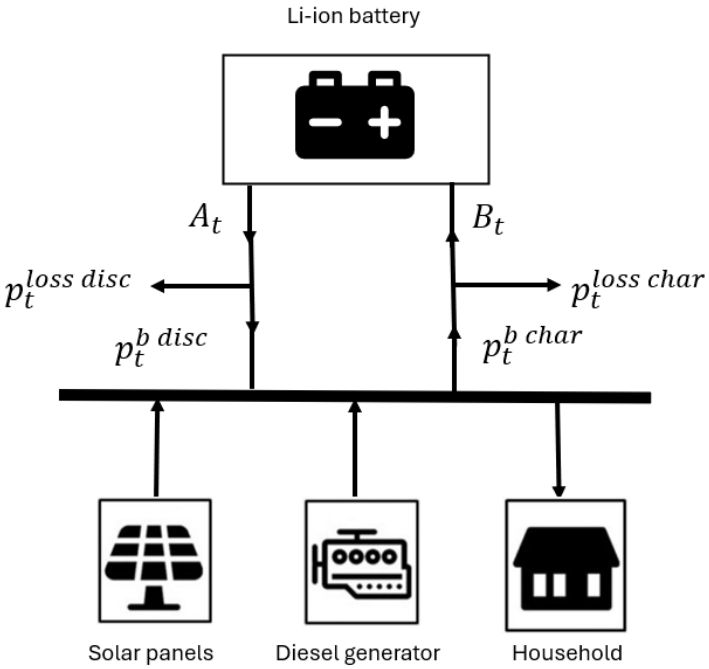


*Figure 2.4: Diagram illustrating power losses in Li-ion battery*

#### 2.4.1.1.1 Discharge

When discharging, the power extracted from the battery ($A_t$) is equal to the sum of the power injected into the microgrid ($p_t^{b\ disc}$) and the power losses ($p_t^{loss\ disc}$):

$$A_t = p_t^{b\ disc} + p_t^{loss\ disc} \tag{2}$$

Moreover, the discharging efficiency of the Li-ion battery ($\eta^{b\ disc}$) is defined as the power injected into the microgrid over the power decrease of the battery storage:

$$\eta^{b\ disc} = \frac{p_t^{b\ disc}}{A_t} \tag{3}$$

When combining equations (2) and (3), the following expression for the power losses when discharging is obtained:

$$p_t^{loss\ disc} = \frac{1 - \eta^{b\ disc}}{\eta^{b\ disc}} p_t^{b\ disc} \tag{4}$$

#### 2.4.1.1.2 Charge

When charging, the power input into the battery ($B_t$) is equal to the power extracted from the microgrid ($p_t^{b\ char}$) minus the power losses ($p_t^{loss\ char}$).

$$B_t = p_t^{b\ char} - p_t^{loss\ char} \tag{5}$$

Moreover, the charging efficiency of the Li-ion battery ($\eta^{b\ char}$) is defined as the power input into the battery over the power extracted from the microgrid.

$$\eta^{b\ char} = \frac{B_t}{p_t^{b\ char}} \tag{6}$$

When combining equations (5) and (6), the following expression for the power losses when charging is obtained:

$$p_t^{loss\ char} = (1 - \eta^{b\ char}) p_t^{b\ char}$$

(7)

### *2.4.1.2 Equations for non-linear losses in Li-ion battery*

To model non-linear losses in the Li-ion battery, the expressions derived in [13] will be used. These equations model power losses as a function of two variables: the state of charge ($soc_t$) and the discharging ($p_t^{b\ disc}$) or charging power ($p_t^{b\ char}$). The state of charge is defined as the charge stored in a particular moment divided by the maximum capacity [13].

These bivariate functions include three parameters that characterize the battery: the rated voltage ($V_r$), the internal resistance ($R$) and the polarization coefficient ($K$). In the microgrid studied, these parameters will take the values shown in Table 2.2.

#### 2.4.1.2.1 Discharge

$$p_t^{loss\ disc} = 10^3 \left(R + \frac{K}{soc_t}\right)\left(\frac{p_t^{b\ disc}}{V_r}\right)^2$$

(8)

#### 2.4.1.2.2 Charge

$$p_t^{loss\ char} = 10^3 \left(R + \frac{K}{1.1 - soc_t}\right)\left(\frac{p_t^{b\ char}}{V_r}\right)^2$$

(9)

# Chapter 3. OPTIMIZATION MODELS

This project proposes two deterministic optimization models for the energy management of the microgrid described in the previous chapter. These models differ in the equations used to calculate the power losses when the Li-ion battery is charging or discharging:

- *LL (Linear Losses)*: Optimization model for the energy management of a microgrid in which linear equations are used to calculate the power losses in the Li-ion battery.
- *NLL (Non-Linear Losses)*: Optimization model for the energy management of a microgrid in which non-linear equations are used to calculate the power losses in the Li-ion battery.

Moreover, two frameworks for the implementation of the optimization models will be proposed:

- *Whole horizon optimization approach*, where the optimization model is solved once for the whole time horizon.
- *Rolling horizon optimization approach*, explained in detail in the following section.

## *3.1 ROLLING HORIZON OPTIMIZATION FRAMEWORK*

The rolling horizon approach is a scheduling method which involves solving an optimization problem in an iterative manner. In each iteration, the optimization model is solved for a predetermined time horizon called prediction horizon. After each iteration, the prediction horizon is moved forward a defined time length (control horizon) along the time horizon studied (scheduling horizon) and the model is solved again. [15] This process is illustrated in Figure 3.1.

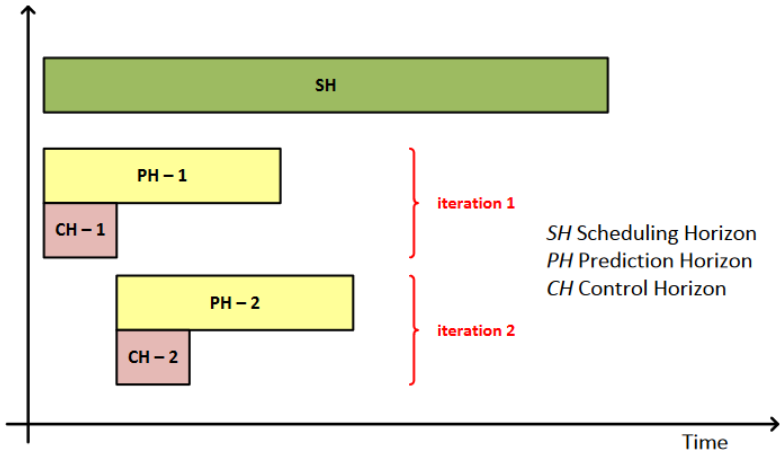


*Figure 3.1: Time horizons in rolling horizon framework (Source: [16])*

The implementation of a rolling horizon framework to solve an optimization problem has multiple advantages. Firstly, a rolling horizon approach is useful when solving problems incorporating a time structure, such as the ones studied in this project, since they are usually very large and, therefore, sometimes cannot be solved to optimality in a reasonable period of time [17]. Decomposing the problem by performing various iterations where the optimization model is solved for smaller time horizons can prove to be advantageous in this aspect. Moreover, solving the optimization problems using a rolling horizon approach allows to emulate what occurs in reality, where data is only available for a limited time horizon and, as time progresses, new data becomes available. Consequently, solving the optimization problems using a rolling horizon framework will provide a better understanding what would be the energy management decisions in a real-life scenario.

To apply the rolling horizon approach to the optimization problems studied in this project, the following algorithm has been developed:

1. Definition of the length of the scheduling horizon ($SH$), the prediction horizon ($PH$) and the control horizon ($CH$)
2. Calculation of the number of iterations ($it$):

$$it = \left\lceil \frac{SH-PH}{CH} + 1 \right\rceil \tag{10}$$

3. Iteration using a For loop for $i = 1$ to $it$.

   3.1. Calculation of initial time period of prediction horizon:

$$t_{ini} = CH(i-1) + 1 \tag{11}$$

   3.2. Calculation of final time period of prediction horizon:

$$t_{fin} = t_{ini} + PH - 1 \tag{12}$$

   3.3. Definition dynamic set $trh$ with the time periods included in the current prediction horizon.

   3.4. Execution of optimization model.

   3.5. Updating of parameters which represent initial states of components. The value assigned will be that of the corresponding time-dependent variable for the time period in which the next prediction horizon starts. In this step it is assumed that the data for which the model is solved is what occurs in reality. This step is illustrated in Figure 3.2.

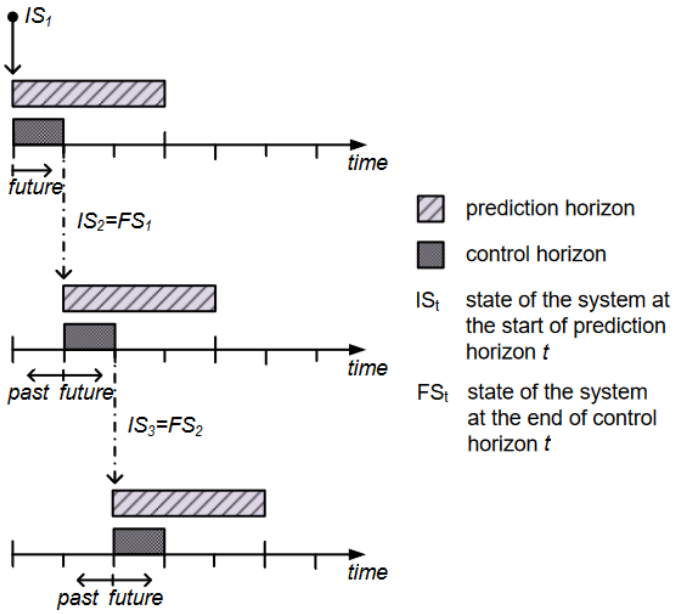


*Figure 3.2: Updating of parameters which represent initial states of components in rolling horizon framework (Source: [16])*

## *3.2 MATHEMATICAL FORMULATION OF OPTIMIZATION MODELS*

In this section, the mathematical formulation of models *LL* and *NLL* will be presented. This formulation includes the sets, parameters, objective function and constraints necessary to define the operation of the components connected to the microgrid studied as well as the interaction between them. Moreover, the classical optimization problem formulation has been adapted to adjust to the implementation of the rolling horizon framework algorithm explained in the previous section.

### 3.2.1 SETS

$t$: time periods in scheduling horizon

$trh$: time periods included in current prediction horizon

### 3.2.2 PARAMETERS

$DT$: duration of time period [h]

$CH$:length of control horizon [h]

$PH$:length of prediction horizon [h]

$SH$:length of scheduling horizon [h]

$it$: number of iterations

$t_{ini}$: initial time period (included) of prediction horizon

$t_{fin}$: final time period (included) of prediction horizon

$C_{nse}$: cost of non-supplied energy [€/kWh]

#### *3.2.2.1 Load*

$D_t$: power demanded by load in period t [kW]

#### *3.2.2.2 Solar Panel*

$PV_t$: power generated by PV panel in period t [kW]

#### *3.2.2.3 Diesel generator*

$a$: quadratic term of diesel generator cost-function [€/kW$^2$h]

$b$: linear term of the diesel generator cost-function [€/kWh]

$c$: independent term of the diesel generation cost-function when the generator is committed [€/h]

$P^d_{max}$: maximum output power of diesel generator [kW]

#### *3.2.2.4 Li-ion battery*

$\eta^{b\ char}$: efficiency of Li-ion battery when charging

$\eta^{b\ disc}$: efficiency of Li-ion battery when discharging

$P^d_{\max char}$: Maximum charge power of Li-ion battery [kW]

$P^d_{\max disc}$: maximum discharge power of Li-ion battery [kW]

$E^b_0$: initial energy stored in Li-ion battery [kWh]

$E^b_{max}$: Maximum energy storage of Li-ion battery [kWh]

$V_r$: rated voltage of battery [V]

$R$: internal resistance of battery [Ω]

K: polarization coefficient [Ω]

### 3.2.3 VARIABLES

$p_t^{ns}$: non-supplied power in period t [kW]

#### *3.2.3.1 Solar panel*

$p_t^{PV}$: power output of solar panel [kW]

$p_t^{curt}$: PV curtailment in period t [KW]

#### *3.2.3.2 Diesel generator*

$u_t^d$: commitment of diesel generator in period t {0,1}

$p_t^d$: power output of diesel generator in period t [kW]

#### *3.2.3.3 Li-ion battery*

$u_t^{b\ char}$: battery charge decision in period t {0,1}

$u_t^{b\ disc}$: battery discharge decision in period t {0,1}

$p_t^{b\ char}$: power consumed by Li-ion battery in period t [kW]

$p_t^{b\ disc}$: power generated by Li-ion battery in period t [kW]

$p_t^{loss\ char}$: power loss of Li-ion battery if charging in period t [kW]

$p_t^{loss\ disc}$: power loss of Li-ion battery if discharging in period t [kW]

$e_t^b$: energy stored in Li-ion battery at the end of period t [kWh]

$soc_t$: state of charge of Li-ion battery in period t [p.u.]

### 3.2.4 OBJECTIVE FUNCTION

The objective of the model is to minimize the total cost of operating the microgrid, which is calculated as the sum of the cost curve for diesel generator, defined in equation (1), and the cost incurred due to the non-supplied energy. Note that the duration of each time step is one hour.

$$min \sum_{t} \left[ a\left(p_t^d\right)^2 + bp_t^d + cu_t^d + c_{nse}p_t^{ns} \right] DT \tag{13}$$

### 3.2.5 CONSTRAINTS

Constraints (14) – (20) and (23) – (30) are used in model *LL* and constraints (14) – (18) and (21) – (30) are used in model *NLL*.

Energy balance of microgrid:

$$p_t^{PV} + p_t^d + p_t^{b\,disc} + p_t^{ns} = D_t + p_t^{b\,char} \quad \forall t \in trh \tag{14}$$

#### *3.2.5.1 Solar panel*

Possible curtailment of power generated by solar panel:

$$PV_t = p_t^{PV} + p_t^{curt} \quad \forall t \in trh \tag{15}$$

#### *3.2.5.2 Diesel generator*

Maximum power diesel generator can generate:

$$p_t^d \leq P_{max}^d u_t^d \quad \forall t \in trh \tag{16}$$

### *3.2.5.3 Li-ion battery*

Battery dynamics:

$$e_t^b = \begin{cases} E_0^b + \left[p_t^{b\ char} - p_t^{loss\ char} - p_t^{b\ disc} - p_t^{loss\ disc}\right]DT & if\ t = t_{ini} \\ e_{t-1}^b + \left[p_t^{b\ char} - p_t^{loss\ char} - p_t^{b\ disc} - p_t^{loss\ disc}\right]DT & if\ t > t_{ini} \end{cases} \quad \forall t \in trh$$

(17)

Approximation of state of charge for each period, where the average value between its instantaneous values at the beginning and at the end of the hour is proposed.

$$soc_t = \begin{cases} \dfrac{\frac{1}{2}\left(E_0^b + e_t\right)}{E_{max}^b} & if\ t = t_{ini} \\ \dfrac{\frac{1}{2}\left(e_{t-1}^b + e_t\right)}{E_{max}^b} & if\ t > t_{ini} \end{cases} \quad \forall t \in trh$$

(18)

Linear expression for power losses in Li-ion battery when charging, based on equation (7):

$$p_t^{loss\ char} = p_t^{b\ char}(1 - \eta^{b\ char}) \quad \forall t \in trh$$

(19)

Linear expression for power losses in Li-ion battery when discharging, based on equation (4):

$$p_t^{loss\ disc} = p_t^{b\ disc}\frac{1 - \eta^{b\ disc}}{\eta^{b\ disc}} \quad \forall t \in trh$$

(20)

Non-linear expression for power losses in Li-ion battery when charging, based on equation (9):

$$p_t^{loss\ char} = 10^3 \left(R + \frac{K}{1.1 - soc_t}\right)\left(\frac{p_t^{b\ char}}{V_r}\right)^2 \quad \forall t \in trh$$

(21)

Non-linear expression for power losses in Li-ion battery when charging, based on equation (8):

$$p_t^{loss\ disc} = 10^3 \left(R + \frac{K}{soc_t}\right)\left(\frac{p_t^{b\ disc}}{V_r}\right)^2 \quad \forall t \in trh$$

(22)

Maximum power Li-ion battery can consume when charging:

$$p_t^{b\ char} \leq P_{max\ char}^{b} u_t^{b\ char} \quad \forall t \in trh$$

(23)

Maximum power Li-ion battery can generate when discharging:

$$p_t^{b\ disc} \leq P_{max\ disc}^{b} u_t^{b\ disc} \quad \forall t \in trh$$

(24)

Battery cannot charge and discharge at the same time:

$$u_t^{b\ char} + u_t^{b\ disc} \leq 1 \quad \forall t \in trh$$

(25)

Maximum state of charge of Li-ion battery:

$$soc_t \leq 1 \quad \forall t \in trh \tag{26}$$

Minimum state of charge of Li-ion battery:

$$soc_t \geq 0.1 \quad \forall t \in trh \tag{27}$$

Maximum energy storage of Li-ion battery:

$$e_t \leq E^b_{max} \quad \forall t \in trh \tag{28}$$

#### *3.2.5.4 Non-negativity and binary*

$$p^{ns}_t,\ p^{PV}_t, p^{curt}_t, p^{d}_t, p^{b\ char}_t, p^{b\ disc}_t, p^{loss\ char}_t, p^{loss\ disc}_t, e^b_t,\ soc_t \geq 0 \quad \forall t \in trh \tag{29}$$

$$u^d_t, u^{b\ char}_t, u^{b\ disc}_t \in \{0,1\} \quad \forall t \in trh \tag{30}$$

## *3.3 CODING OF OPTIMIZATION MODELS*

General Algebraic Modelling System (GAMS) has been used to code both optimization models *LL* and *NLL*. GAMS is a high-level algebraic modelling language used extensively to develop decision support models. It is widely used in fields such as Energy Production, Manufacturing, Logistics, Engineering and Economics for formulating and solving

mathematical optimization problems due to its ability to handle large-scale and complex problems efficiently [12]. The code developed for this project is included in Appendix I and has been implemented within a single .gms file where the user can select which model to execute.

# Chapter 4. GAMS SOLVERS

Within the GAMS system, multiple solvers are available depending on the type of optimization problem to be solved. Using the most appropriate solver is crucial to reaching the optimal solution and achieving the best computational performance.

*LL* is a mixed integer quadratic programming model due to the objective function being quadratic and the use of binary variables to specify the commitment of the diesel generator and whether the Li-ion battery is charging or discharging. In GAMS, this type of optimization model falls within the category of mixed integer quadratically constrained program (MIQCP) and it will be solved using GUROBI. This solver has been chosen instead of CPLEX due to its superior performance in a similar optimization problem solved in [13], which was confirmed during trial runs in the model validation stage.

*NLL* contains non-linearities as well as integer variables. In addition to the quadratic objective function and the binary variables in model *LL*, non-linear terms are present in the constraints used to model power losses when the Li-ion battery is charging or discharging. Given these characteristics of the optimization problem, it is considered to fall within the category of mixed integer non-linear problems (MINLP).

MINLP is frequently considered a “difficult” category of optimization problems due to the presence of both integer variables as well as non-linear functions, requiring a framework which addresses both by combining the capabilities of mixed-integer linear programming (MILP) and nonlinear programming (NLP) [18]. This requires the use of solvers different from those considered for model *LL*, such as CPLEX and GUROBI.

Solver performance is highly dependent of the optimization problem being solved [19]. In fact, it is practically impossible to predict which solvers will be capable of solving a certain model and which will demonstrate a superior performance [20]. This implies that testing is required to identify the most suitable solver for a given optimization problem [12].

This project will focus on testing and evaluating two MINLP solvers: DICOPT and BARON. Sections 4.1 and 4.2 will cover each solver separately, aiming to provide an overview of their characteristics based on the information provided by GAMS manuals for DICOPT [20] and BARON [21] and relevant papers regarding these algorithms, such as [22]. The following sections will cover why these solvers have been selected, basing this decision on their performance when solving a variety of MINLP problems in previous literature as well as their intrinsic differences when approaching the resolution of MINLP problems. Furthermore, even though the algorithms used by the solvers and the theory behind them is beyond the scope of this project, they will be briefly described to better illustrate the differences between the solvers and facilitate the understanding of solver options. Additionally, an explanation of the solver options relevant to this project will be provided.

## *4.1 DICOPT*

DICOPT (Discrete Continuous Optimizer) is a program used to solve MINLP problems originally developed at the Engineering Design Research Center (EDRC) in Carnegie Mellon University by Jagadisan Viswanathan, Ignacio E. Grossmann, and Aldo Vecchietti.

This solver was selected due to its proven outstanding efficiency and performance in previous literature. For instance, in [19], when compared to other MINLP solvers in time usage in 89 problems, it has the lowest average execution time. Moreover, it offers a wide range of optimization capabilities through its integration with other solvers which will be discussed further on in more detail. DICOPT is also a versatile solver given its ability to solve both convex and non-convex problems. Nevertheless, it is important to note that, even though the solver is equipped to handle non-convexities, it does not necessarily obtain the global optimum.

DICOPT's approach to solving MINLP problems involves the alternate resolution of mixed integer programming (MIP) and non-linear programming (NLP) sub-problems. Firstly, the algorithm begins by solving a relaxed version of the specified problem in which binary

variables are allowed to take continuous values between 0 and 1. The resulting optimization problem falls within the NLP category. If in the solution obtained the binary variables take integer values, the search ends. If not an alternating sequence of MIP master problems and NLP subproblems is executed. Each iteration of the sequence begins by solving a MIP problem which is based on the outer-approximation/equality-relaxation algorithm. An exact penalty function is used to allow violations of linearizations of non-convex constraints. After the MIP master problem has been solved, an NLP sub-problem is solved. This NLP problem is obtained through fixing binary variables with the values from the MIP master problem's solution. The iterative process stops when the optimal value of the objective function for an NLP sub-problem is worse than the one of the previous NLP sub-problem.

To solve the MIP and NLP sub-problems, any solver which runs under GAMS can be used. The performance of DICOPT will greatly depend on the sub-solvers selected so choosing the most appropriate ones for the model studied is crucial to achieve a successful implementation. However, it is difficult, especially for NLP problems, to know in advance how well a solver will perform. Consequently, an objective of this project will be to analyze the impact of the non-linear solver chosen on the computational performance and the energy management of the microgrid for model *NLL*. By using the DICOPT options *mipsolver* and *nlpsolver*, combinations of the following sub-solvers will be tested:

- MIP solvers: GUROBI
- NLP solvers: CONOPT, IPOPT, MINOS and SNOPT

By default, DICOPT solves MIP sub-problems to optimality. However, when models have many integer variables, it is sometimes necessary to use the *optcr* option to ensure that the model is solved in a reasonable amount of time. This is known as the relative optimality criterion and it causes the solver to stop as soon as the best solution found minus the best possible solution all divided by the best possible solution is smaller than a specified value. This value set using a GAMS option file.

Another stopping criterion which can be used is *reslim*, which enables restricting the execution time to a specified wall-clock time limit.

One final option to feature in this section which can prove to be extremely powerful is *relaxed*. By default, *relaxed* is equal to 1 and results in the initial NLP problem being solved with all integer variables relaxed between their bounds. If *relaxed* is set to 0, the initial NLP problem solved is obtained by fixing the integer variables to values set by the user, instead of by relaxing the integer variables. This is useful when the user can provide a known reasonable configuration of the integer variables in the problem. The second option can prove advantageous in tackling highly complex optimization problems, especially when the relaxed problem is unsolvable, but solving NLP sub-problems with fixed integer variables is considerably more manageable. This project can profit from the implementation of this feature since a known configuration for the integer variables in the model can be obtained by solving model *LL* first and feeding the results to the MINLP model *NLL*.

## *4.2 BARON*

BARON (Branch and Reduce Optimization Navigator) is a GAMS solver which can provide the global solution to NLP and MINLP problems. Its algorithm involves the use of constraint propagation, interval analysis, and duality to achieve an efficient range reduction while, through the enlargement of the feasible region and/or underestimation of the objective function, rigorous relaxations are constructed.

The main advantage of solving an optimization problem using BARON is its ability to provide a global optimum under fairly broad assumptions through the use of deterministic global optimization algorithms of the branch-and-bound type. This does not hold true for traditional solvers, such as DICOPT, which are only guaranteed to converge under specific convexity assumptions. Consequently, BARON excels in finding the best possible solutions, ensuring a high level of accuracy in optimization tasks.

Even if BARON stands out for its ability to address non-convex problems through a global approach, it was also identified as one of the most efficient solvers for convex problems by [18], which presents a review of solvers applied to convex MINLP problems. BARON has

showcased superior performance compared to DICOPT in the literature. For instance, in [19] it was able to solve difficult problems to feasibility within 1000 seconds whereas DICOPT found no solution after a few seconds. In addition, when benchmarked against various global solvers in [23], it was concluded that BARON was the fastest and most robust one.

However, it is important to note that these advantages can come at an expense of increased computational times.

Similarly to DICOPT, BARON offers a wide range of optimization capabilities thanks to its integration with other solvers. By default, BARON may switch throughout its execution between available LP/MIP/QP solvers and available NLP solvers. BARON may use the following sub-solvers:

- LP/MIP/QP solvers: CLP/CBC and ILOG CPLEX
- NLP solvers: MINOS, SNOPT, External NLP, IPOPT and FILTERSQP

BARON options *LPSol* and *NLPSol* allow the user to indicate a single specific LP/MIP/QP solver and NLP solver to use. The performance of BARON can vary depending on the solver combinations selected, therefore, in line with the objective mentioned in the previous section of analyzing the impact of the non-linear solver chosen on the computational performance and the energy management of the microgrid for model *NLL*, combinations of the following solver options will be tested:

- LP/MIP/QP solvers: Default (automatic solver selection and switching strategy)
- NLP solvers: Default (automatic solver selection and switching strategy), IPOPT, MINOS and SNOPT

As stopping criteria, *optcr* and *reslim* will be used. In BARON, the definition of *optcr* differs slightly from that of DICOPT. For this solver, *optcr* specifies the relative termination tolerance for the global solver, not for a sub-solver, and is defined as the objective function value of the best feasible solution found up until that moment minus the current bound on the optimal value of the problem all divided by the maximum between these two values.

# Chapter 5. COMPARATIVE ANALYSIS OF OPTIMIZATION MODELS AND SOLVERS

In this chapter, through application to a case study, a comparative analysis of models and solvers will be performed. The aim of the study will be to determine which model-solver combinations yield a better performance and evaluate the differences regarding the energy management for the best-performing combinations.

The models studied will include the following:

- *LL*: Optimization model for the energy management of a microgrid in which linear equations are used to calculate the power losses in the Li-ion battery.
- *NLL*: Optimization model for the energy management of a microgrid in which non-linear equations are used to calculate the power losses in the Li-ion battery.
- *ZZI-J1*: Optimization model presented in [13] for the energy management of a microgrid. This model uses piecewise linear approximations of the non-linear power losses equations implemented using an integer zig-zag (ZZI) formulation. The resulting optimization model is of type MIQCP. Multiple models were presented in [13] using the ZZI formulation but ZZI-J1 8x8 exhibited superior behavior.

The solver used for models *LL* and *ZZ-J1 8x8* will be GUROBI and for *NLL* the following combinations will be tested:

- DICOPT with a relaxed initial NLP (*relaxed* = 1), using GUROBI as the MIP sub-solver and CONOPT, IPOPT, MINOS or SNOPT as the NLP sub-solver.
- DICOPT with fixed binary variables in initial NLP (*relaxed* = 0), using GUROBI as the MIP sub-solver and CONOPT, IPOPT, MINOS or SNOPT as the NLP sub-solver. Binary variables in the initial NLP will be fixed using results obtained from solving *LL* using GUROBI.

- BARON using the default configuration for the MIP sub-solver and MINOS, SNOPT, IPOPT or the default configuration for the NLP sub-solver.

The case study used will consist in a large-scale problem of 168 hours (1 week) using data from [14], as explained in Chapter 2.

A *whole horizon optimization approach* will be employed as the framework for the implementation of the three models, meaning that the optimization model is solved once for the whole time horizon. This can be considered a particular case of the rolling horizon optimization framework developed and coded in GAMS, where the scheduling horizon is equal to the prediction horizon.

The stopping criteria used for all model-solver combinations are a wall-clock time limit of one hour (*reslim* = 3600) and a relative optimality criterion of 0.5% (*optcr* = 0.005).

## *5.1 COMPARATIVE ANALYSIS OF COMPUTATIONAL PERFORMANCE*

Table 5.1 presents the results obtained when executing the model-solver combinations detailed previously. The model-solver performance parameters which will be compared are the best objective function value found, the execution time and the relative gap. Empty cells in the Obj. and Time columns indicate that the solver was unable to find an integer solution within the one-hour time limit. The relative gap was not included for models solved using DICOPT since it refers to the MIP sub-problems, whereas for the other solvers a global relative gap is provided.

| ***Model*** | ***Main Solver*** | ***Relaxed*** | ***MIP Sub-solver*** | ***NLP Sub-solver*** | ***Obj. [€]*** | ***Time [s]*** | ***Rel. Gap*** |
|---|---|---|---|---|---|---|---|
| LL | GUROBI | - | - | - | 5.4197 | 5.69 | 0.32% |
| NLL | DICOPT | 1 | GUROBI | CONOPT | 7.0354 | 3613.14 | - |
| NLL | DICOPT | 1 | GUROBI | IPOPT | - | - | - |
| NLL | DICOPT | 1 | GUROBI | MINOS | 6.9869 | 11.11 | - |
| NLL | DICOPT | 1 | GUROBI | SNOPT | 6.8991 | 6.09 | - |
| NLL | DICOPT | 0 | GUROBI | CONOPT | 4.7509 | 35.47 | - |
| NLL | DICOPT | 0 | GUROBI | IPOPT | 4.7509 | 3631.53 | - |
| NLL | DICOPT | 0 | GUROBI | MINOS | 4.7509 | 23.97 | - |
| NLL | DICOPT | 0 | GUROBI | SNOPT | 4.7510 | 133.20 | - |
| NLL | BARON | - | Default | Default | 4.7421 | 3603.14 | 1.72% |
| NLL | BARON | - | Default | MINOS | 4.7436 | 3602.42 | 1.74% |
| NLL | BARON | - | Default | SNOPT | 4.7426 | 3602.50 | 1.73% |
| NLL | BARON | - | Default | IPOPT | 4.7459 | 3602.27 | 1.79% |
| ZZI-J1 | GUROBI | - | - | - | 4.7526 | 139.53 | 0.38% |

*Table 5.1: Summary of computational performance of model-solver combinations*

For the models which consider non-linear losses in the Li-ion battery (*NNL* and *ZZI-J1*), based on the best solutions found across the model-solver combinations, the optimal value of the objective function for the case studied seems to be approximately between 4.7€ and 4.8€ per week.

Table 5.1 shows that, when solving model *NLL* using DICOPT with a relaxed initial NLP, the value of the objective function for all NLP sub-solvers tested is around 7€. This value is notably greater than the approximate optimal value for the case studied. Consequently, it can

be concluded that the DICOPT is converging towards a local optimum and is unable to reach the global optimum. This implies that the optimization problem studied is non-convex and, even though DICOPT is equipped to handle non-convexities, it does not necessarily obtain the global optimum.

This issue is overcome when solving model *NLL* using DICOPT with fixed binary variables in the initial NLP. In Table 5.1 it can be observed that, for all solver combinations within this category, the model is converging towards the global optimum given that the objective function values lie between 4.7€ and 4.8€. Hence, for the MINLP model proposed in this project, aiding the MINLP solver by providing it with a known reasonable configuration of the integer variables in the problem, which in this case is the optimal solution obtained by the linear model *LL*, results in a successful outcome.

When solving model *NLL* using BARON, the solution also converges towards the global optimum. This highlights BARON's main strength as a global solver, which allows it to provide a global optimum under fairly broad conditions and not only under certain convexity assumptions.

GUROBI solves optimization problems to global optimality subject to a specific optimality tolerance specified by the user. This can be seen in the objective function value obtained when using model *ZZI-J1*.

It is noteworthy to mention that the objective function value for model *LL*, which considers linear losses in the Li-ion battery, is approximately 0.6€ greater than the previously suggested upper bound of the optimal value of the objective function for models which consider non-linear losses. The reason behind this is not that GUROBI is converging towards a local optimum but the fact that the linear and non-linear formulations cannot be considered equivalent since different parameters are used in the power losses equations.

Consequently, whether the objective function value of the non-linear model is smaller or greater than the one obtained using the linear model will depend on the parameters used to characterize the Li-ion battery. In section 5.2, a possible approach to making parameters

used in the linear model equivalent to those used in the non-linear model will be explored and its impact on the results obtained analyzed.

Although model *LL* does not seem directly comparable from the point of view of the objective function value, in terms of execution time it outperforms all other models. This stands as a clear advantage of modeling losses in the Li-ion battery as linear in the energy management of a microgrid. However, to further understand the differences between modeling power losses as linear versus non-linear, it will be interesting to analyze and compare the results obtained from an energy management perspective.

Overall, the lowest objective function values are achieved when using BARON, specifically when the default option is used for both the MIP sub-solver and the NLP sub-solver. This model-solver combination would lead to the lowest microgrid operating costs. Moreover, it can be concluded that for the model developed in this project, using the default options for both sub-solvers, which allows BARON to switch between the ones available, results in a superior performance.

For the model-solver combinations analyzed in this project, the relative gap does not enable a global comparison since it is defined differently for each solver. However, this parameter can be used to compare model *NLL* solved using BARON and model *ZZI-J1*. The latter has a lower relative gap which means that the final solution provided by the solver is closer to the best possible solution when the execution ends. Model *NLL* solved using BARON was unable to reach a lower relative gap since the time limit was reached.

Regarding the execution time of models considering non-linear losses, DICOPT showcases a wide range of execution times, emphasizing the importance of the sub-solver selection. Considering only the DICOPT combinations that converged towards a global optima, the lowest execution time was achieved when MINOS was used as NLP sub-solver. It is worth noting that Model *ZZI-J1* is solved in a very competitive time frame as well. On the other hand, BARON showed the lowest performance in this aspect since it reached the one-hour time limit for all sub-solver combinations.

Amongst the models which consider non-linear losses in the Li-ion battery, the one which showcases the best performance when considering both the objective function value and the execution time is *NLL* when solved using DICOPT with fixed binary variables in the initial NLP, specifically when GUROBI is used as the MIP sub-solver and MINOS is used as the NLP sub-solver.

## *5.2 SENSITIVITY ANALYSIS*

As mentioned in the previous section, the linear and non-linear formulations cannot be considered completely equivalent since different parameters are used in the power losses equations. A possible approach to making these parameters equivalent would be determining the average operation efficiency for the period studied. To do this, the results provided by the *NLL*-BARON combination with the default sub-solver configurations were used.

To calculate an estimation of the average operation efficiency, the instantaneous efficiencies for each time period were obtained and a weighted average based on the charging/discharging power calculated. The results obtained were a charging and discharging efficiency of approximately 99%.

As a sensitivity analysis for the case study proposed, the model-solver combinations detailed previously were re-tested using a charging and discharging efficiency of 99%, instead of 90%. The results obtained are shown in Table 5.2.

| ***Model*** | ***Main Solver*** | ***Relaxed*** | ***MIP Sub-solver*** | ***NLP Sub-solver*** | ***Obj. [€]*** | ***Time [s]*** | ***Rel. Gap*** |
|---|---|---|---|---|---|---|---|
| LL | GUROBI | - | - | - | 4.7530 | 5.66 | 0.40% |
| NLL | DICOPT | 1 | GUROBI | CONOPT | 7.0354 | 3613.14 | - |
| NLL | DICOPT | 1 | GUROBI | IPOPT | - | - | - |
| NLL | DICOPT | 1 | GUROBI | MINOS | 6.9869 | 11.11 | - |
| NLL | DICOPT | 1 | GUROBI | SNOPT | 6.8991 | 6.09 | - |
| NLL | DICOPT | 0 | GUROBI | CONOPT | 4.7393 | 164.05 | - |
| NLL | DICOPT | 0 | GUROBI | IPOPT | 4.7393 | 3147.75 | - |
| NLL | DICOPT | 0 | GUROBI | MINOS | 4.7393 | 94.20 | - |
| NLL | DICOPT | 0 | GUROBI | SNOPT | 4.7393 | 1154.16 | - |
| NLL | BARON | - | Default | Default | 4.7421 | 3603.14 | 1.72% |
| NLL | BARON | - | Default | MINOS | 4.7436 | 3602.42 | 1.74% |
| NLL | BARON | - | Default | SNOPT | 4.7426 | 3602.50 | 1.73% |
| NLL | BARON | - | Default | IPOPT | 4.7459 | 3602.27 | 1.79% |
| ZZI-J1 | GUROBI | - | - | - | 4.7526 | 127.81 | 0.38% |

*Table 5.2: Summary of computational performance for sensitivity analysis*

The model-solver combinations affected by this change are *LL*-GUROBI, given that the linear losses equations include the charging/discharging efficiency, and *NLL*-DICOPT with fixed binary variables in initial NLP, since these binary variables are fixed based on the results of *LL*-GUROBI.

When comparing Tables 5.1 and 5.2, it can be seen that the objective function value of *LL*-GUROBI now does fall between 4.7€ and 4.8€, where the global optimum when modeling losses as non-linear seems to be located. In addition, the objective function values for all

*NLL*-DICOPT combinations with fixed binary variables in the initial NLP have improved. However, the execution time when using sub-solvers MINOS and SNOPT has increased.

Although this could be suggesting that this method improves the performance of *NLL*-DICOPT with fixed binary variables in the initial NLP and makes *LL*-GUROBI more comparable, the real-life applicability and hence validity of this procedure is debatable.

The reason for this is that average efficiency depends on the case study analyzed. Different load and PV generation profiles lead to a different optimal microgrid energy management strategies which may result in higher or lower average efficiencies. Consequently, if the average efficiency obtained for this case study were to be used with other datasets, it is likely that it would imply an overestimation or underestimation. Given this possible caveat in the method, the comparative analysis of the energy management in the following chapter will be done using the base case results.

Modeling losses as non-linear is more realistic and, therefore, more accurate results will be obtained to fulfill the power demand for a given solar generation profile. This will imply lower operation costs if efficiency was being underestimated and possibly less unserved power if it was being overestimated. Furthermore, even if the impact of considering non-linear losses as opposed to linear losses might seem small for a single microgrid, the advantages become clear when considering the aggregate impact of millions of microgrids.

Overall, the analyses presented in this section highlight the disadvantages of using a model which considers linear losses.

## *5.3 COMPARATIVE ANALYSIS OF ENERGY MANAGEMENT*

The objective of this section is to analyze how the best-performing sub-solver combination for each model and main solver optimize the energy management in the microgrid studied in the project.

Figures 5.1, 5.3, 5.5 and 5.7 show the results obtained for the operation of the microgrid components for each model-solver combination. Moreover, to graphically illustrate how demand is fulfilled in the 168-hour time period, stacked area charts are presented in Figures 5.2, 5.4, 5.6 and 5.8.

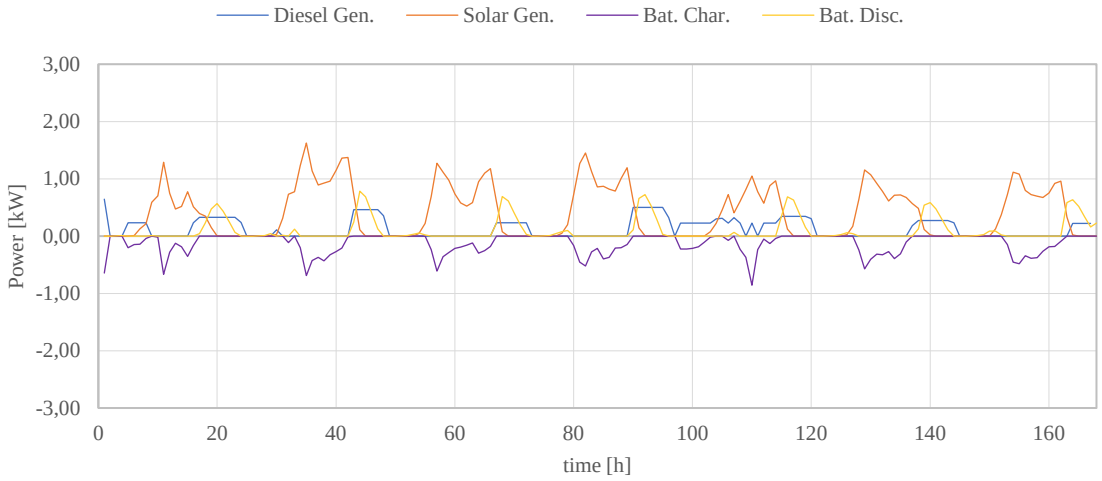


*Figure 5.1: Operation of microgrid components (LL, GUROBI, 168 hours)*

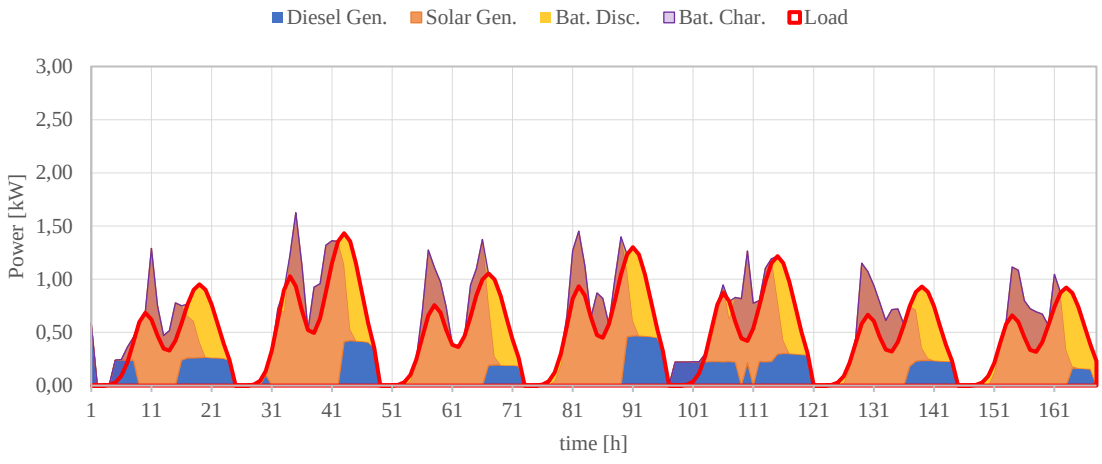


*Figure 5.2: Demand fulfillment (LL, GUROBI, 168 hours)*

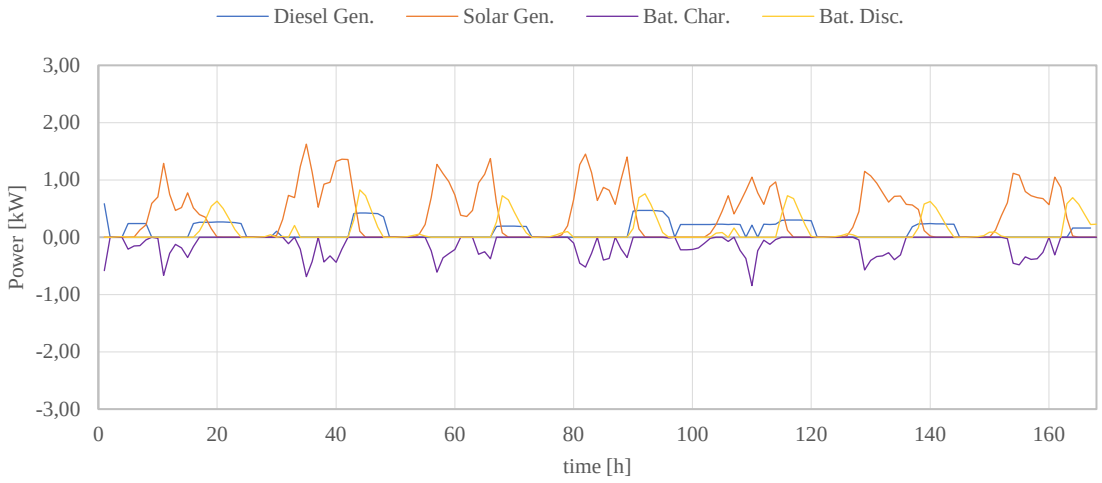


*Figure 5.3: Operation of microgrid components (NLL, DICOPT, relaxed=0, GUROBI-MINOS, 168 hours)*

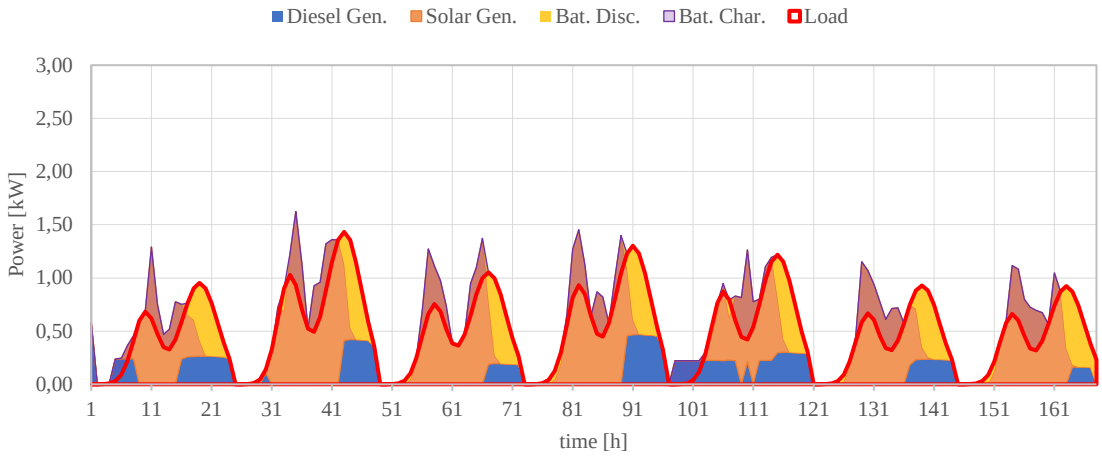


*Figure 5.4: Demand fulfillment (NLL, DICOPT, relaxed=0, GUROBI-MINOS, 168 hours)*

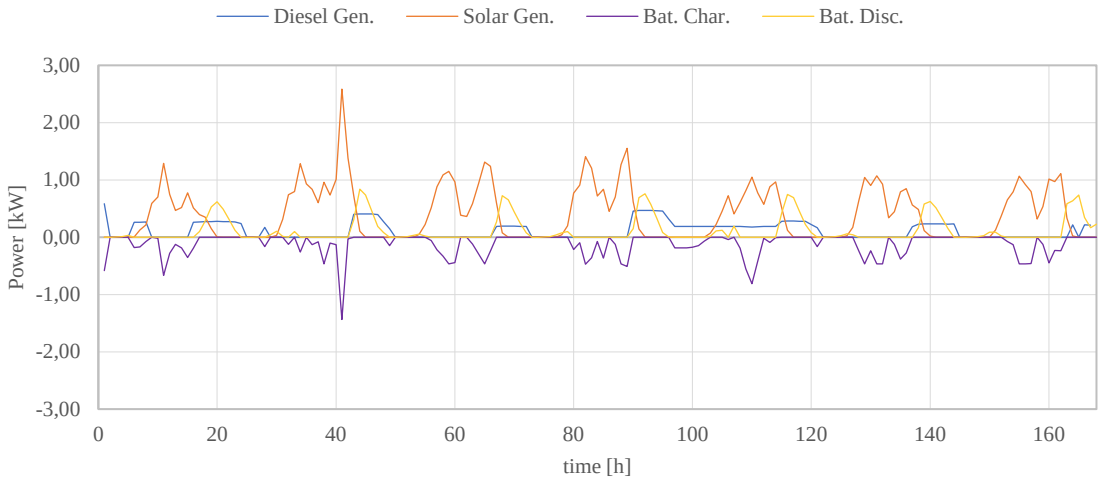


*Figure 5.5: Operation of microgrid components (NLL, BARON, Default-Default, 168 hours)*

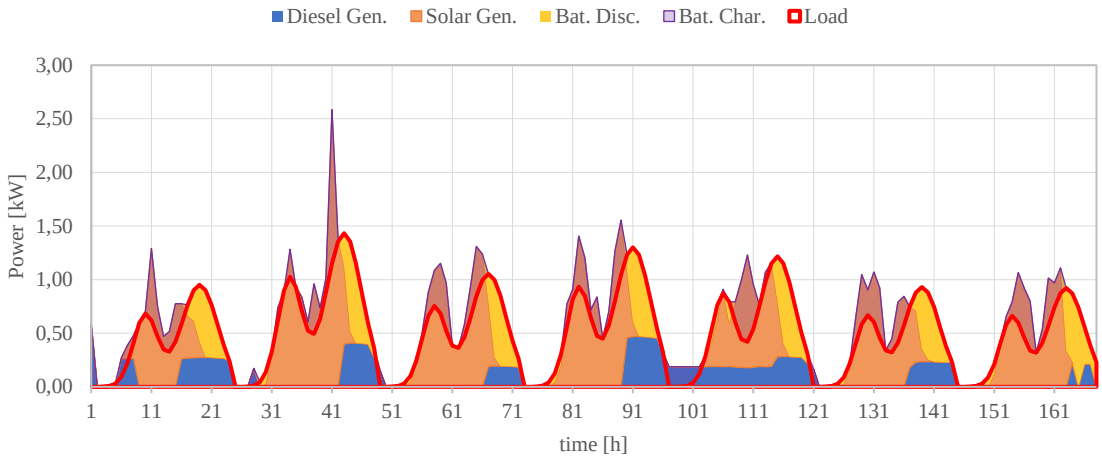


*Figure 5.6: Demand fulfillment (NLL, BARON, Default-Default, 168 hours)*

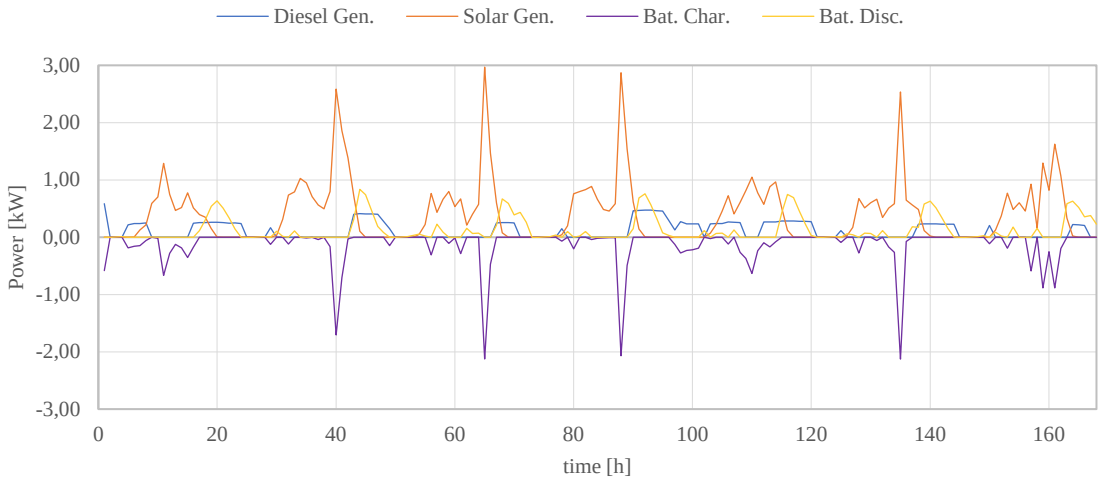


*Figure 5.7: Operation of microgrid components (ZZI-J1, GUROBI, 168 hours)*

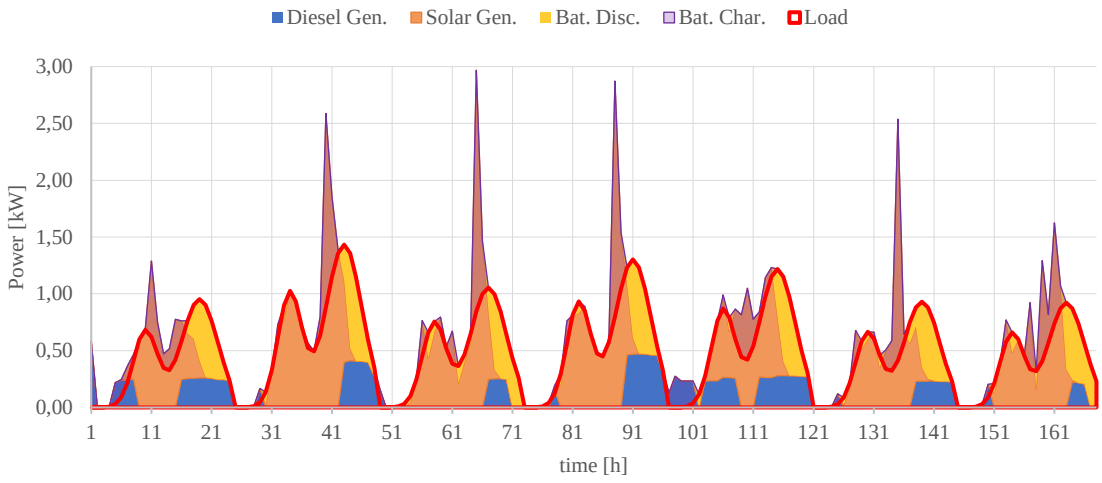


*Figure 5.8: Demand fulfillment (ZZI-J1, GUROBI, 168 hours)*

The graphs show a pattern in the daily energy management strategy for the microgrid across all the model-solver combinations. Energy provided during the daylight hours is used to fill the Li-ion battery and the battery charging power peak occurs during the solar generation peak. During the evening, the battery discharges to fulfill the demand peak. At the beginning

of the time period, the controller dispatches a small amount of diesel power since the Li-ion battery's SoC it at its minimum. Usually, the diesel generator is on during demand peaks in the evening since the level of solar radiation is low and battery can't supply all the power demanded on its own. However, on day 5, since the solar irradiation is lower than the rest of the days, consequently, the diesel generator supplies power practically throughout the whole day.

To allow a more accurate comparison between the models, in the following sections the most relevant variables which characterize the operation of the microgrid components will be studied separately.

### 5.3.1 SOLAR PANEL

The solar panel power output varies depending on the PV power available. On days with less sunlight, such as days 1 and 5, the solar panel supplies the microgrid with all the PV power available in all model-solver combinations. However, when more sunlight is available, the energy management strategies of the model-solver combinations analyzed differ. Figure 5.5 shows that *ZZI-J1* supplies solar power to the microgrid in a less uniform way than other models, presenting very pronounced peaks and deeper valleys.

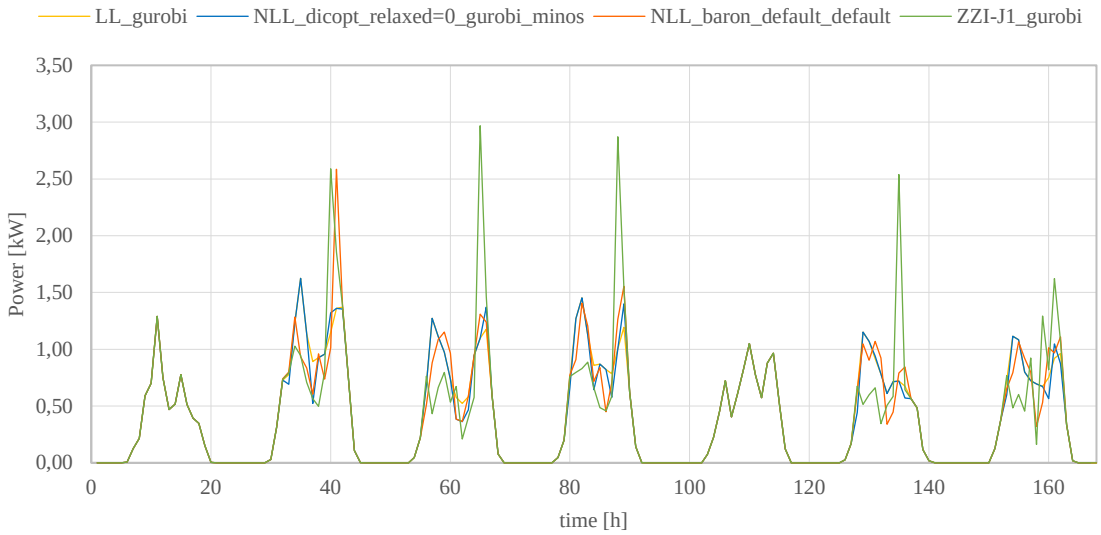


*Figure 5.9: Obtained results (Solar Gen., 168 hours)*

### 5.3.2 LI-ION BATTERY

The main variables regarding the operation of the Li-ion battery include: the charging/discharging power, the charging/discharging power losses, and the state of charge.

When looking at Figure 5.6, although days 1 and 5 seem very similar for all model-solver combinations, on the rest of the days, model *ZZI-J1* presents very high charging peaks during the hours with most sunlight. Initially it might seem that the best energy management strategy is to make the most out of the sunlight peaks. However, when the Li-ion battery operates at a very high power, the power losses are very high too, as illustrated in Figure 5.7.

*NLL*-BARON also exhibits a peak of high power losses (Figure 5.7) that corresponds to a peak in the Li-ion battery charging power (Figure 5.6).

Figure 5.7 clearly shows that the total power losses of model *LL* are the highest amongst all model-solver combinations depicted. This is due to the efficiency used to characterize the Li-ion battery (90%) being lower than the average efficiency showcased by models which consider non-linear losses (approximately 99%).

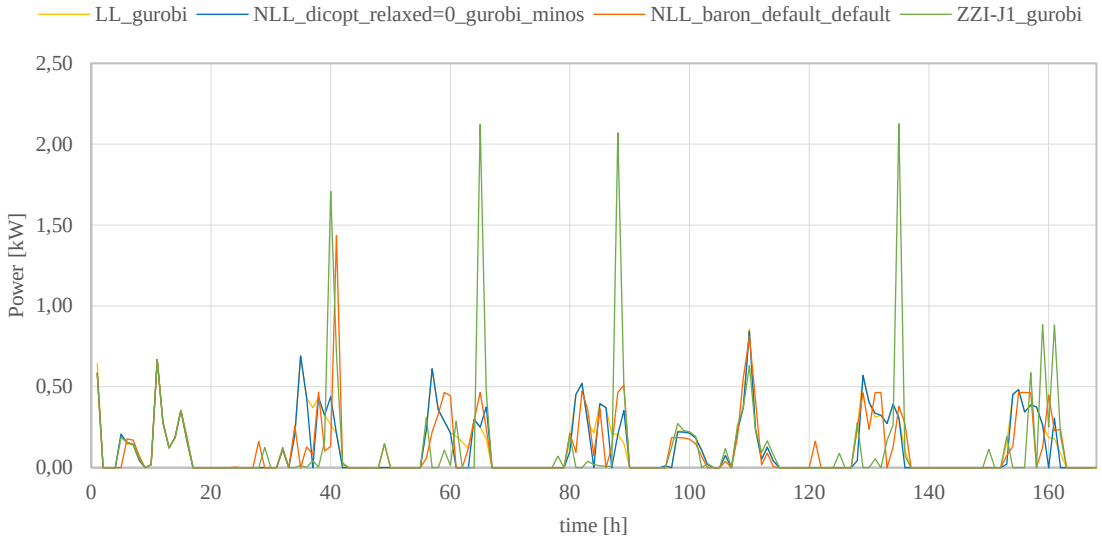


*Figure 5.10: Obtained results (Bat. Char., 168 hours)*

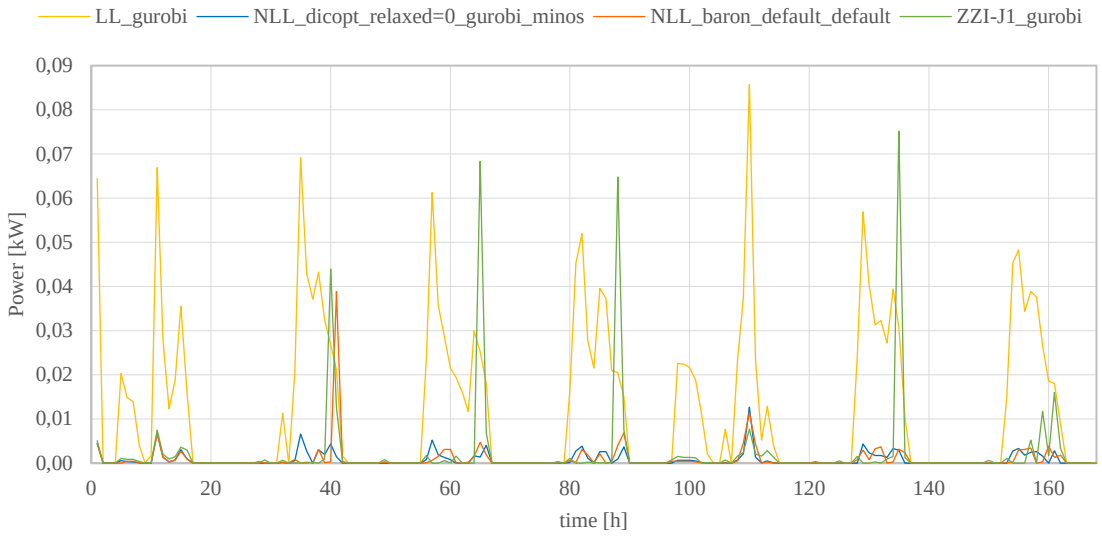


*Figure 5.11: Obtained results (Losses Bat. Char., 168 hours)*

Battery discharging power does not present much variation between model-solver combinations, as shown in Figure 5.8.

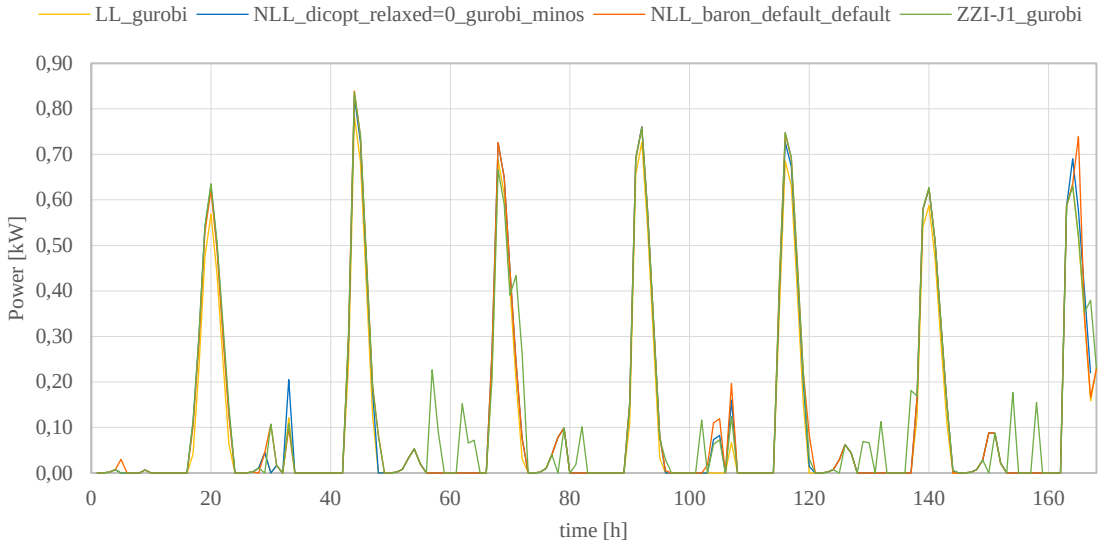


*Figure 5.12: Obtained results (Bat. Disc., 168 hours)*

Discharging power losses (Figure 5.9) are only noticeably different for model *LL* due to the efficiency used to characterize the Li-ion battery, as mentioned before.

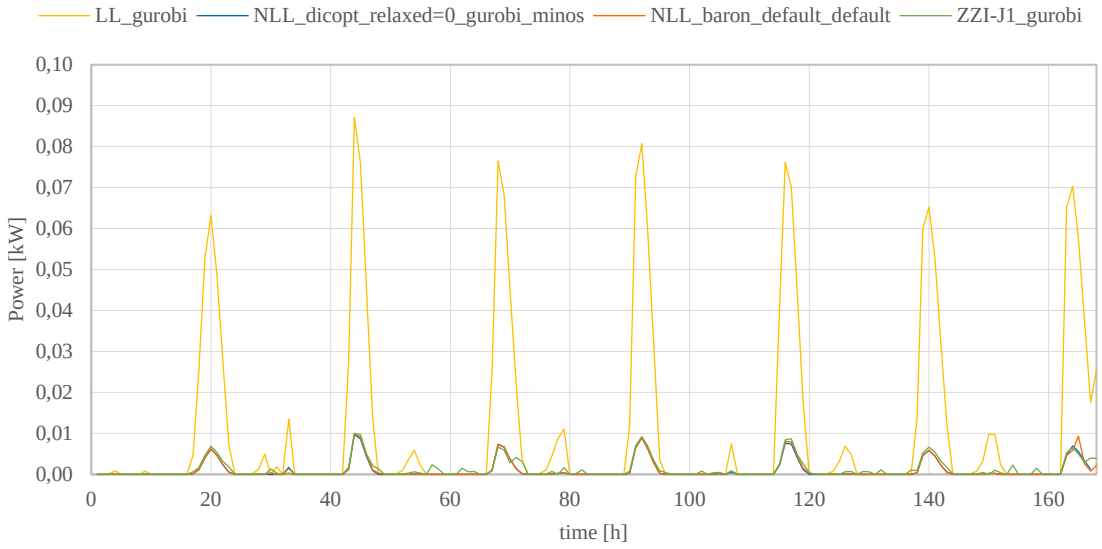


*Figure 5.13: Obtained results (Losses Bat. Disc., 168 hours)*

When analyzing the state of charge of the battery using Figure 5.10, on certain days, model *ZZI-J1* presents a more abrupt charging of the battery than the other model-solver combinations due to the very pronounced charging peaks shown in Figure 5.6.

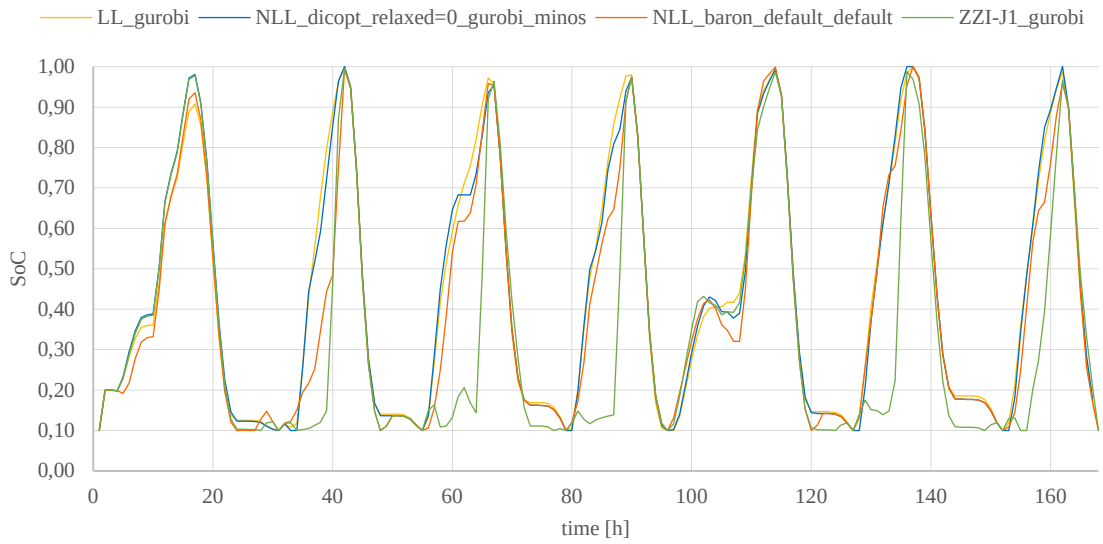


*Figure 5.14: Obtained results (SoC, 168 hours)*

### 5.3.3 DIESEL GENERATOR

The diesel generator is the only component in the microgrid whose operation incurs in a cost. The *NLL*-BARON combination is the one than uses diesel power the least and, therefore, achieves the lowest objective function value amongst all the model-solver combinations compared. Consequently, *NLL*-BARON's strategy of using solar energy in a more uniform manner along the day is more optimal than *ZZI-J1*'s strategy. This is due to higher battery charging power implying higher charging power losses which have to be compensated using diesel power.

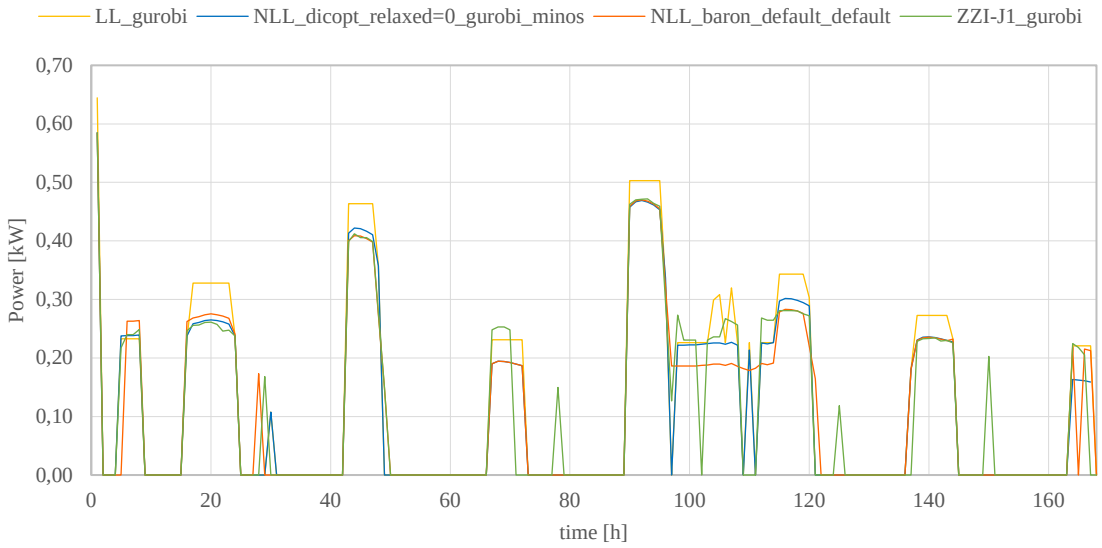


*Figure 5.15: Obtained results (Diesel Gen., 168 hours)*

# Chapter 6. IMPLEMENTATION OF ROLLING HORIZON OPTIMIZATION FRAMEWORK

Based on the results analyzed in Chapter 5, *NLL*-BARON has showcased a superior performance in terms of the objective function value. Compared to all other model-solver combinations studied, it obtained the lowest objective function values and had the potential to lower them even further if allowed more time.

However, a main drawback of using *NLL*-BARON is its lengthy execution time, since the one-hour time limit was reached for all sub-solver combinations. To address this, the implementation of a *rolling horizon optimization approach*, presented in Chapter 3, will be explored in this chapter.

This will be done by executing *NLL*-BARON with the default sub-solver configurations for two 168-hour datasets, one corresponding to a week in summer and the other one corresponding to a week in winter, using a *whole horizon optimization approach* and a *rolling horizon optimization approach*. The time horizons used in the rolling framework are shown in Table 6.1.

| ***Time horizon*** | ***Time length [h]*** |
|---|---|
| Scheduling horizon | 168 |
| Prediction horizon | 24 |
| Control horizon | 8 |

*Table 6.1: Time horizons used the in rolling horizon approach*

These time horizon parameters result in 19 iterations in which the model is solved for 24-hour periods. For each iteration, the prediction horizon is moved forward 8 hours. Figures 6.1 and 6.2 illustrate the rolling horizon dynamic for the case studied.

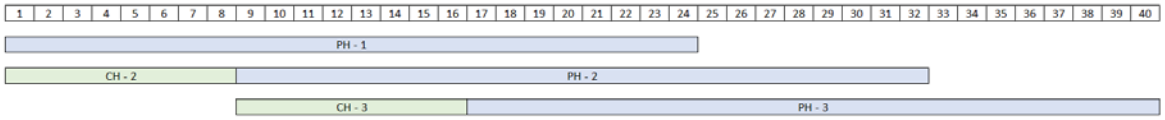


*Figure 6.1: Time horizons for time periods 1-40*

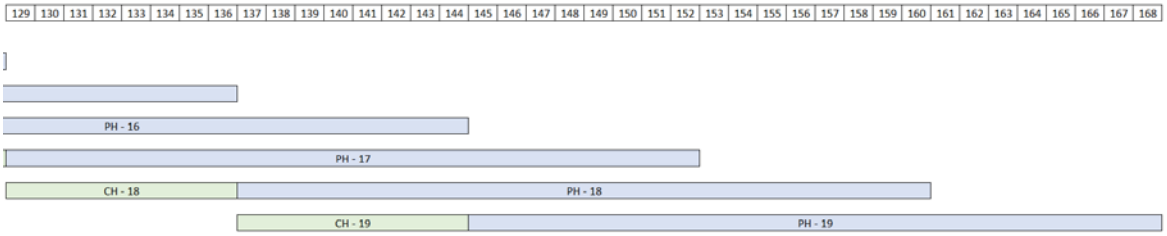


*Figure 6.2: Time horizons for periods 129-168*

## 6.1 COMPARATIVE ANALYSIS OF COMPUTATIONAL PERFORMANCE

Table 6.2 presents the results obtained for each dataset-optimization approach combination. From these results, it can be concluded that using a *rolling horizon optimization approach* decreases execution time and improves the objective function value. This supports the findings of paper [17] discussed in Chapter 3.

| ***Dataset*** | ***Optimization approach*** | ***Obj. [€]*** | ***Time [s]*** |
|---|---|---|---|
| Summer | Whole horizon | 4.7421 | 3603.14 |
| Summer | Rolling Horizon | 4.7251 | 1524.06 |
| Winter | Whole horizon | 19.0309 | 765.69 |
| Winter | Rolling Horizon | 19.0190 | 578.50 |

*Table 6.2: Summary of computational performance of NNL-BARON*

Regarding the summer dataset, the decrease in the objective function value could be attributed to the fact that BARON is able to reach lower relative tolerances when solving a sequence of smaller sub-problems instead of one large optimization problem. The relative tolerances achieved for each rolling horizon iteration were all smaller that the relative optimality criterion used (0.5%), whereas, when using the whole horizon approach, the resulting relative tolerance was 1.74%, as shown in Table 5.1.

Moreover, the BARON configuration used is flexible in terms of the sub-solvers chosen. This could be leading to the selection of solvers which are better suited for the smaller sub-problems defined by the rolling horizon approach. Consequently, this would be contributing to achieving lower execution times and objective function values.

It is important to note that the selection of an appropriate prediction horizon length greatly impacts how successful the implementation of a rolling horizon framework is [15]. For the optimization problem studied in this project, using a 24-hour prediction horizon leads to an improvement in computational performance compared to using a *whole horizon approach* meaning this time-window length appears appropriate for the problem.

## 6.2 COMPARATIVE ANALYSIS OF ENERGY MANAGEMENT

The objective of this section is to determine whether there are differences in energy management strategies between summer and winter and analyze how energy management differs when using a *whole horizon optimization approach* versus a *rolling horizon optimization approach.*

### 6.2.1 SEASONAL DIFFERENCES IN ENERGY MANAGEMENT

To examine the differences in energy management between winter and summer, the results obtained using *rolling horizon optimization approach* will be compared. Figures 6.3 and 6.5 illustrate the operation of the microgrid components and Figures 6.4 and 6.5 show how the different power sources are used to fulfill demand.

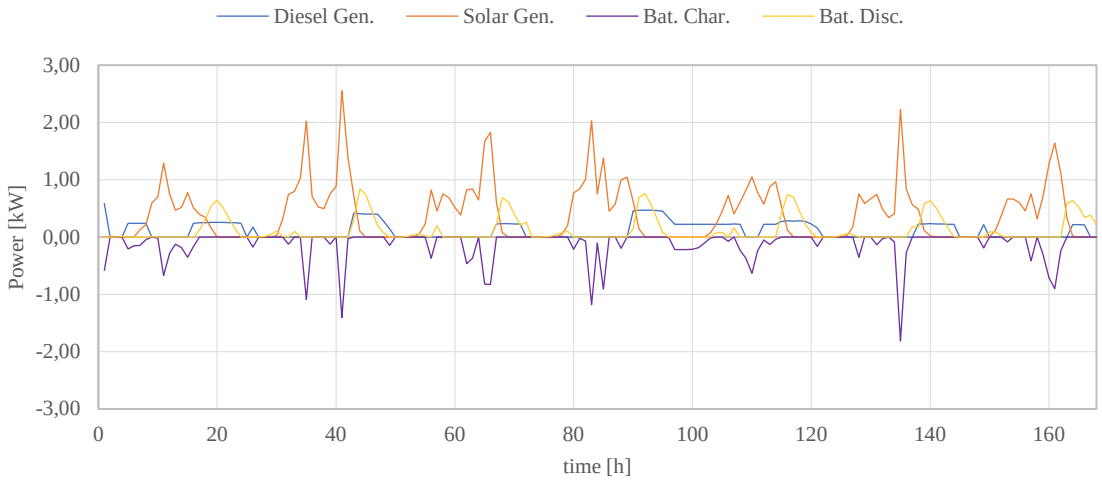


*Figure 6.3: Operation of microgrid components (NLL-BARON, 168 hours Summer, Rolling horizon)*

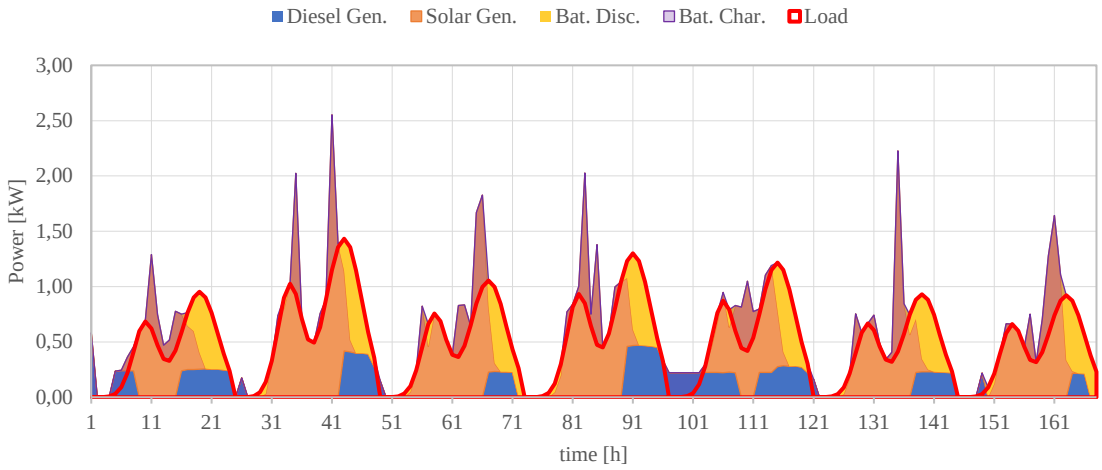


*Figure 6.4: Demand fulfillment (NLL-BARON, 168 hours Summer, Rolling horizon)*

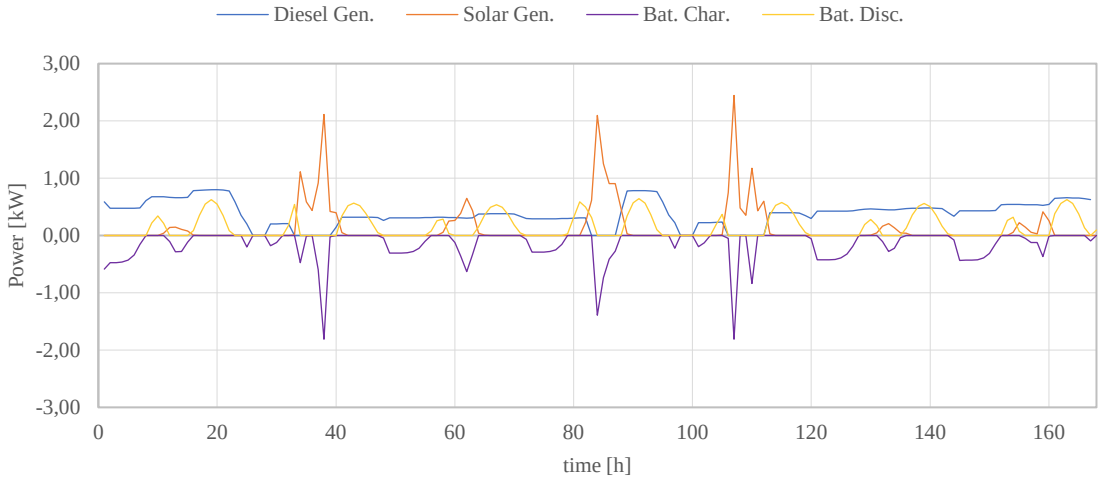


*Figure 6.5: Operation of microgrid components (NLL-BARON, 168 hours Winter, Rolling horizon)*

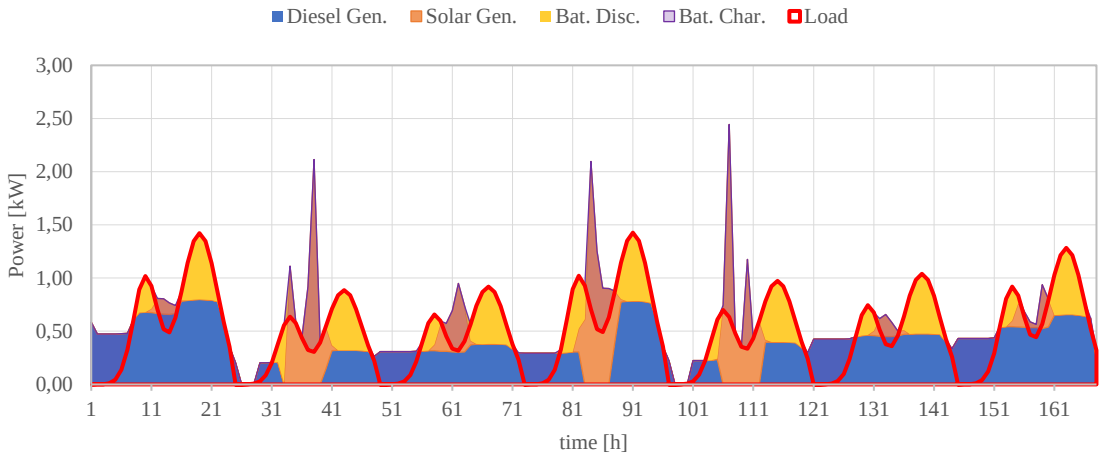


*Figure 6.6: Demand fulfillment (NLL-BARON, 168 hours Winter, Rolling horizon)*

No major differences can be observed in the load profile between summer and winter. However, the variation in solar irradiation, and hence the solar generation, does differ noticeably and is the key factor that determines the variation in operation strategy between the seasons.

In both seasons, the battery takes advantage of the solar generation peaks to charge. Regarding discharging patterns, in winter the battery discharges during both peaks in demand whereas in summer it mostly discharges during the largest peak in demand since the other peak occurs when there is a medium level of solar generation which helps meet demand.

In winter, the diesel generator plays a much more important role since it is needed practically throughout the entire day. It charges the battery during off-peak hours so this power can be used later on and compensates for the lack of solar irradiation by helping the battery fulfill demand during peak hours. In contrast, during summer, the use of the diesel generator is practically limited to supporting the battery during the highest daily demand peak.

### 6.2.2 DIFFERENCES IN ENERGY MANAGEMENT BETWEEN OPTIMIZATION APPROACHES

The main difference between both optimization approaches is that the *rolling horizon optimization approach* uses slightly more solar generation than the *whole horizon optimization approach* (Figures 6.3 and 6.4). This implies a lower diesel generation usage (Figures 6.5 and 6.6), which leads to lower overall operation costs.

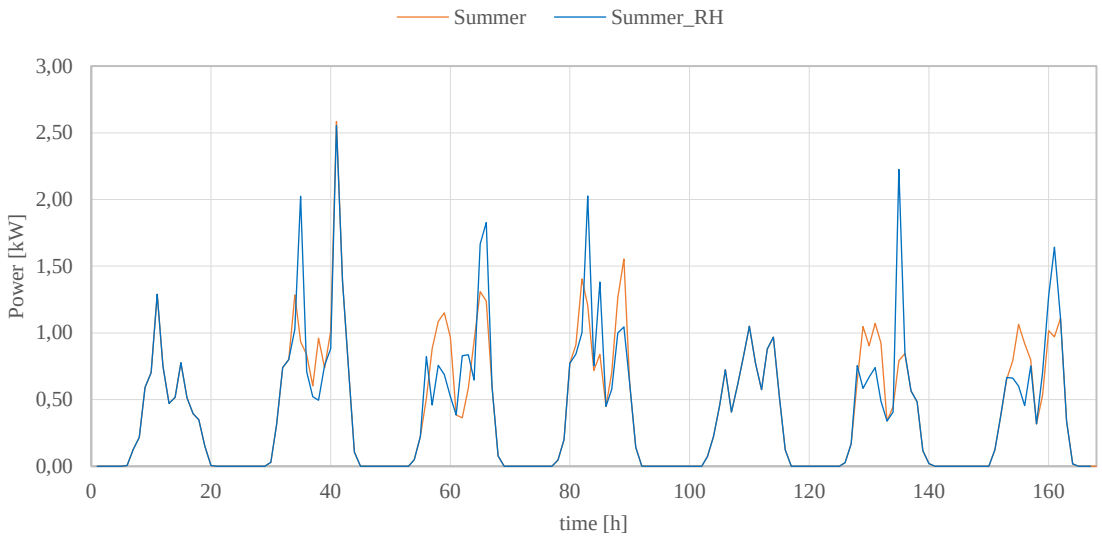


*Figure 6.7: Demand fulfillment (NLL-BARON, 168 hours Winter, Rolling horizon)*

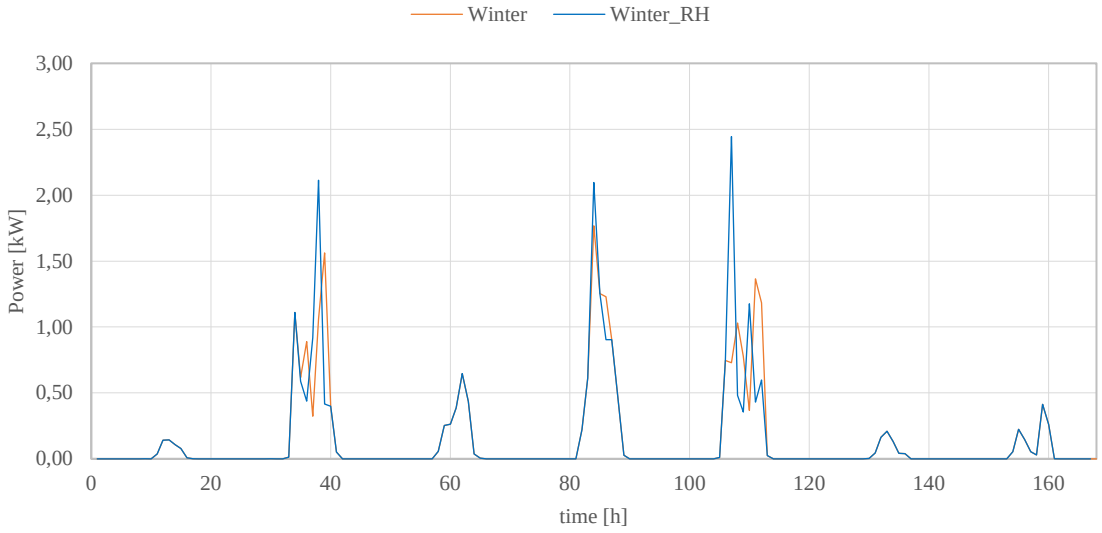


*Figure 6.8: Obtained results (Solar Gen., NLL-BARON, 168 hours Winter)*

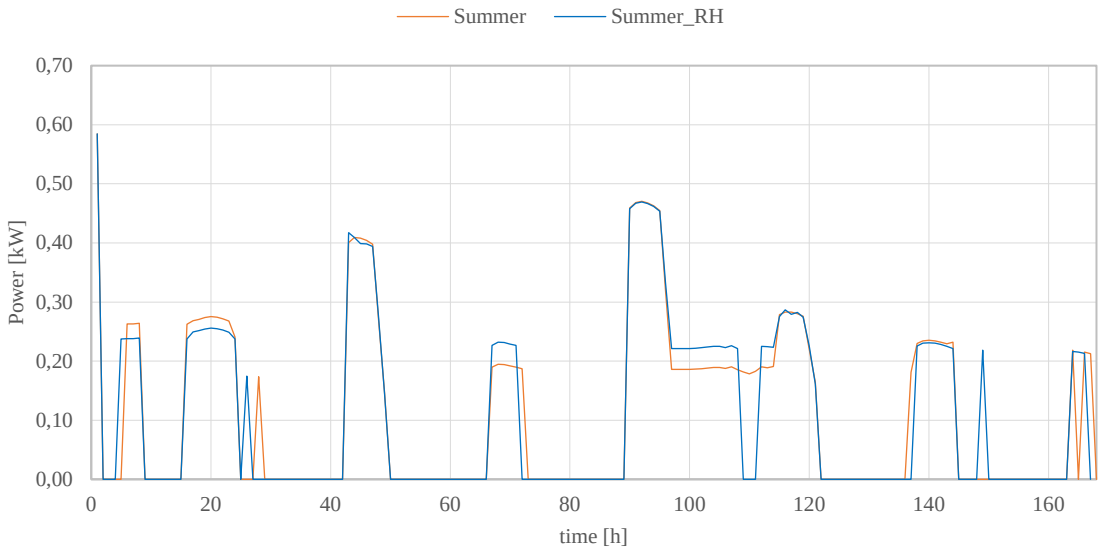


*Figure 6.9: Obtained results (Solar Gen., NLL-BARON, 168 hours Winter)*

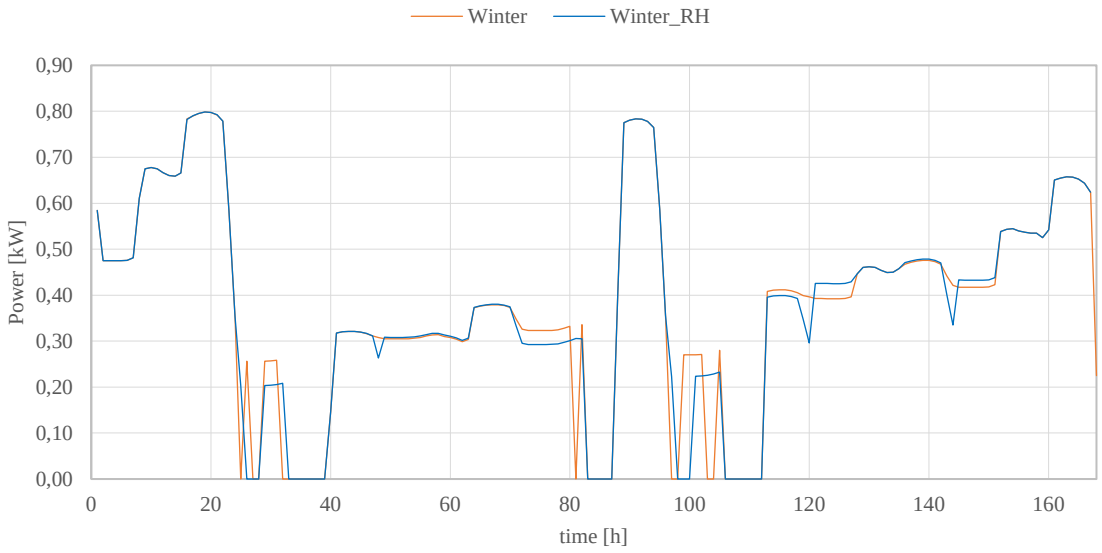


*Figure 6.10: Obtained results (Diesel Gen., NLL-BARON, 168 hours Winter)*

Additional graphs for other variables have been included in Appendix II.

# Chapter 7. CONCLUSIONS

## *7.1 CONCLUSIONS*

In this project, two optimization models for the energy management of a microgrid consisting of a load, a solar panel, a diesel generator, and a lithium-ion battery have been developed, one considering linear losses in the Li-ion battery (model *LL*) and another one considering non-linear losses (model *NLL*).

These models, together with model *ZZI-J1* proposed in [13], have been tested using different GAMS solvers and solver configurations for a 168-hour dataset and applying a *whole horizon optimization approach*. Solver BARON was able to find the global optimum whereas DICOPT converged towards a local optimum unless the binary variables in the problem were fixed using results obtained from solving model *LL*. Regarding computational performance, in terms of the objective function value (weekly operation cost), *NLL*-BARON, specifically when the default configuration for the sub-solvers was used, showcased a superior performance. However, when looking at the execution time, BARON performed worse than the other solvers tested. Overall, the model which had the best computational performance considering both the execution time and the objective function value was *NLL*-DICOPT with fixed binary variables in the initial NLP, specifically when MINOS was used as the NLP sub-solver. This highlights the benefits of providing a known reasonable configuration of the binary variables in the problem.

Analyses carried out concluded that modeling losses as linear can lead to underestimating the average efficiency of the Li-ion battery implying higher operation costs. This highlights a clear drawback of using a model which considers linear losses.

Furthermore, in this project, a rolling horizon framework was developed and tested for the best-performing *NLL*-BARON model-solver combination. This optimization approach improved its computational performance decreasing both the objective function value

(weekly operation cost) and execution time. Moreover, this implementation served as a simulation of the real-life operation of a microgrid and how it affects energy management.

Overall, the results obtained have shown a successful performance when using an optimization model which considers non-linear losses in the Li-ion battery. Therefore, this project contributes to the increase in accuracy and effectiveness of microgrid energy management, ultimately reducing operation costs and increasing power supply reliability.

## *7.2 FUTURE WORK*

Given the promising results of model *NLL*, this model could be transformed from deterministic to stochastic to account for the uncertainty in solar power generation and household power demand. An interesting approach would involve the implementation of the rolling horizon framework developed in this project to allow for the continual adjustment of scenarios as new information becomes available.

Future investigations could also analyze the impact of changing parameters of microgrid components on model performance. This could provide further insights into the influence of modeling losses as non-linear in the Li-ion battery for a variety of microgrid types and sizes. Linked with this, it would be valuable to explore the consequences of modeling losses as non-linear when scaling to industrial microgrids or applied to large batteries installed in the transmission network to provide flexibility in power systems with high RES penetration levels.

# Chapter 8. BIBLIOGRAPHY

[1] Thirunavukkarasu, G. S., Seyedmahmoudian, M., Jamei, E., Horan, B., Mekhilef, S., & Stojcevski, A. (2022). Role of optimization techniques in microgrid energy management systems—A review. *Energy Strategy Reviews*, *43*, 100899. https://doi.org/10.1016/j.esr.2022.100899

[2] IEA (2022), Renewables 2022, IEA, Paris https://www.iea.org/reports/renewables-2022

[3] IEA (2023), Electricity Market Report 2023, IEA, Paris https://www.iea.org/reports/electricity-market-report-2023

[4] Akinyele, D., Belikov, J., & Levron, Y. (2018). Challenges of Microgrids in Remote Communities: A STEEP Model Application. *Energies*, *11*(2), Article 2. https://doi.org/10.3390/en11020432

[5] Domínguez-Barbero, D., García-González, J., & Sanz-Bobi, M. Á. (2023). Twin-delayed deep deterministic policy gradient algorithm for the energy management of microgrids. *Engineering Applications of Artificial Intelligence*, *125*, 106693. https://doi.org/10.1016/j.engappai.2023.106693

[6] Ali, A., Li, W., Hussain, R., He, X., Williams, B. W., & Memon, A. H. (2017). Overview of Current Microgrid Policies, Incentives and Barriers in the European Union, United States and China. *Sustainability*, *9*(7), Article 7. https://doi.org/10.3390/su9071146

[7] Shahzad, S., Abbasi, M. A., Ali, H., Iqbal, M., Munir, R., & Kilic, H. (2023). Possibilities, Challenges, and Future Opportunities of Microgrids: A Review. *Sustainability*, *15*(8), Article 8. https://doi.org/10.3390/su15086366

[8] Salehi, N., Martínez-García, H., Velasco-Quesada, G., & Guerrero, J. M. (2022). A Comprehensive Review of Control Strategies and Optimization Methods for Individual and Community Microgrids. *IEEE Access*, *10*, 15935–15955. https://doi.org/10.1109/ACCESS.2022.3142810

[9] Allwyn, R. G., Al-Hinai, A., & Margaret, V. (2023). A comprehensive review on energy management strategy of microgrids. *Energy Reports*, *9*, 5565–5591. https://doi.org/10.1016/j.egyr.2023.04.360

[10] Chaouachi, A., Kamel, R. M., Andoulsi, R., & Nagasaka, K. (2013). Multiobjective Intelligent Energy Management for a Microgrid. *IEEE Transactions on Industrial Electronics*, *60*(4), 1688–1699. https://doi.org/10.1109/TIE.2012.2188873

[11] Alavi, S. A., Ahmadian, A., & Aliakbar-Golkar, M. (2015). Optimal probabilistic energy management in a typical micro-grid based-on robust optimization and point estimate method. *Energy Conversion and Management*, *95*, 314–325. https://doi.org/10.1016/j.enconman.2015.02.042

[12] *GAMS - Cutting Edge Modeling*. (n.d.). Retrieved 13 January 2024, from https://www.gams.com/

[13] García-González, J., & Guerrero, S. (2024). Optimal management of a microgrid Li-Ion battery considering non-linear losses using the Integer Zig-Zag formulation. *23rd Power Systems Computation Conference.*

[14] François-Lavet, V., & Taralla, D. DeeR. (2016). Available online: http://deer.readthedocs.io (accessed on 15 February 2024).

[15] Silvente, J., Kopanos, G. M., Pistikopoulos, E. N., & Espuña, A. (2015). A rolling horizon optimization framework for the simultaneous energy supply and demand planning in microgrids. *Applied Energy*, *155*, 485–501. https://doi.org/10.1016/j.apenergy.2015.05.090

[16] Silvente, J., Kopanos, G. M., Dua, V., & Papageorgiou, L. G. (2018). A rolling horizon approach for optimal management of microgrids under stochastic uncertainty. *Chemical Engineering Research and Design*, *131*, 293–317. https://doi.org/10.1016/j.cherd.2017.09.013

[17] Glomb, L., Liers, F., & Rösel, F. (2022). A rolling-horizon approach for multi-period optimization. *European Journal of Operational Research*, *300*(1), 189–206. https://doi.org/10.1016/j.ejor.2021.07.043

[18] Kronqvist, J., Bernal, D. E., Lundell, A., & Grossmann, I. E. (2019). A review and comparison of solvers for convex MINLP. *Optimization and Engineering*, *20*(2), 397–455. https://doi.org/10.1007/s11081-018-9411-8

[19] Lastusilta, T., Bussieck, M. R., & Westerlund, T. (n.d.). *Comparison of Some High-Performance MINLP Solvers*.

[20] *DICOPT*. (n.d.). Retrieved 16 May 2024, from https://www.gams.com/latest/docs/S_DICOPT.html

[21] *BARON*. (n.d.). Retrieved 16 May 2024, from https://www.gams.com/latest/docs/S_BARON.html

[22] Viswanathan, J., & Grossmann, I. E. (1990). A combined penalty function and outer-approximation method for MINLP optimization. *Computers & Chemical Engineering*, *14*(7), 769–782. https://doi.org/10.1016/0098-1354(90)87085-4

[23] Neumaier, A., Shcherbina, O., Huyer, W., & Vinkó, T. (2005). A comparison of complete global optimization solvers. *Mathematical Programming*, *103*(2), 335–356. https://doi.org/10.1007/s10107-005-0585-4

[24] United Nations (n.d.). *THE 17 GOALS | Sustainable Development*. Retrieved 16 February 2024, from https://sdgs.un.org/goals

# APPENDIX I. GAMS CODE

```
* Energy Management of a Microgrid Considering Non-Linear Losses in the Li-ion
Battery
* María del Carmen García Pardo

* OPTIONS

* Solver selection
*OPTIONS LP=CPLEX, RMIP=CPLEX, MIP=CPLEX, RMIQCP=CPLEX, MIQCP=CPLEX;
OPTIONS LP=gurobi, RMIP=gurobi, MIP=gurobi, RMIQCP=gurobi, MIQCP=gurobi;

*OPTIONS MINLP=dicopt;
OPTIONS MINLP=baron;

* Other options
OPTIONS LIMROW=1000, LIMCOL=1000, SOLPRINT=on;
OPTIONS THREADS=0;
OPTIONS RESLIM=3600;
*OPTIONS ITERLIM=2000000;
OPTIONS bratio=1;
OPTION  optcr=0.005;


SETS

t time intervals included in imported data
/h05041*h05208/
trh(t) time intervals included in current prediction horizon
;

* Import data
parameter PV(t) power generated by PV panel at time period t [kW]
/
$include genPV_168h.txt
/
;

parameter D(t) power demanded by load at time period t [kW]
/
$include load_168h.txt
/
;

* Reduce demand profile by 30% to reduce the amount of non-served power
D(t)=D(t)*0.7;


PARAMETERS
```

```
DT Duration of time interval [h] /1/

* Rolling horizon
CH length of control horizon [h] /8/
PH length of prediction horizon [h] /24/
SH length of scheduling horizon [h] /168/
it iteration
t_ini initial time period (included) of prediction horizon
t_fin final time period (included) of prediction horizon
v_ofv_RH objective function value for whole scheduling horizon

* Non-supplied energy:
c_nse cost of non-supplied energy [€ per KWh] /1/

* Diesel generator:
a quadratic term of diesel generator cost-function [€ per kW^2h] /0.31/
b linear term of the diesel generator cost-function [€ per kWh] /0.108/
c independent term of the diesel generator cost function when the generator is
committed [€ per h] /0.0157/

P_d_max maximum output power of diesel generator [kW] /1/

* Li-ion battery:
eta_b_char efficiency of Li-ion battery when charging /0.99/
eta_b_disc efficiency of Li-ion battery when discharging /0.99/


P_b_max_char maximum charge power of Li-ion battery [kW] /2.9/
P_b_max_disc maximum discharge power of Li-ion battery [kW] /2.9/

E_b_0 initial energy stored in Li-ion battery [kWh] /0/
E_b_max maximum energy storage of Li-ion battery [kWh] /2.9/


V_r rated voltage of Li-ion battery [V] /51.2/
R internal resistance of battery [ohm] /0.026464/
K polarization coefficient [ohm] /0.0080625/
;


VARIABLES
v_ofv objective function value [€]
;

POSITIVE VARIABLES

v_p_ns(t) non-supplied power in t [kW]

* Solar panel:
v_p_pv(t) power output of solar panel [kW]
v_p_curt(t) PV curtailment in t [kW]
```

```
* Diesel generator:
v_p_d(t) power output of diesel generator in t [kW]

* Li-ion battery:
v_p_b_char(t) power consumed by Li-ion battery in t [kW]
v_p_b_disc(t) power generated by Li-ion battery in t [kW]

v_p_loss_char(t) power loss of Li-ion battery if charging at time t [kW]
v_p_loss_disc(t) power loss of Li-ion battery if discharging at time t [kW]

v_e_b(t) energy stored in Li-ion battery at the end of t [kWh]
v_soc(t) state of charge of Li-ion battery at time period t
;

* Bounds of the variables
v_soc.lo(t)=0.1;
v_soc.up(t)=1;
v_e_b.up(t)=E_b_max

BINARY VARIABLES

* Diesel generator:
v_u_d(t) commitment of diesel generator in t

* Li-ion battery
v_u_b_char(t) battery charge decision at time t
v_u_b_disc(t) battery discharge decision at time t
;


EQUATIONS
eq_OF objective function: minimize cost of operating microgrid

eq_ENERGY_BALANCE(t) energy balance of microgrid


* Li-ion battery:
eq_BATTERY_DYNAMICS(t) dynamics of Li-ion battery considering losses in Li-ion
battery
eq_SOC(t) approximation of state of charge

* Constraints for model with LINEAR LOSSES
eq_BATTERY_LOSSES_CHAR_LINEAR(t) linear expression for power losses in Li-ion
battery when charging
eq_BATTERY_LOSSES_DISC_LINEAR(t) linear expression for power losses in Li-ion
battery when discharging

* Constraints for model with NON-LINEAR LOSSES
eq_BATTERY_LOSSES_CHAR_NONLINEAR(t) non-linear expression for power losses in Li-
ion battery when charging
eq_BATTERY_LOSSES_DISC_NONLINEAR(t) non-linear expression for power losses in Li-
ion battery when discharging
```

```
eq_BATTERY_MAX_CHAR(t) maximum power Li-ion battery can consume when charging
eq_BATTERY_MAX_DISC(t) maximum power Li-ion battery can generate when discharging
eq_BATTERY_CHAR_OR_DISC(t) battery cannot charge and discharge at the same time

* Diesel generator:
eq_DIESEL_MAX_GEN(t) maximum power diesel generator can generate


* Solar panel:
eq_PV_CURT(t) possible curtailment of power generated by solar panel

;

eq_OF..
    v_ofv =E= SUM[trh(t),c*v_u_d(t) + b*v_p_d(t) + a*sqr(v_p_d(t)) +
c_nse*v_p_ns(t)] * DT;


eq_ENERGY_BALANCE(trh(t))..
    v_p_pv(t) + v_p_d(t) + v_p_b_disc(t) + v_p_ns(t) =E= D(t) + v_p_b_char(t);


* Li-ion battery:
eq_BATTERY_DYNAMICS(trh(t))..
    v_e_b(t) =E= E_b_0$(t.ord=t_ini)+  v_e_b(t-1)$(t.ord > t_ini) +
(v_p_b_char(t) - v_p_b_disc(t) - v_p_loss_disc(t) - v_p_loss_char(t))*DT;

eq_SOC(trh(t))..
    v_soc(t) =E= (1/2) * (E_b_0$(t.ord=t_ini)+  v_e_b(t-1)$(t.ord > t_ini) +
v_e_b(t)) / E_b_max;

* Constraints for model with LINEAR LOSSES
eq_BATTERY_LOSSES_CHAR_LINEAR(trh(t))..
    v_p_loss_char(t) =E=  v_p_b_char(t) * (1-eta_b_char);

eq_BATTERY_LOSSES_DISC_LINEAR(trh(t))..
    v_p_loss_disc(t) =E= v_p_b_disc(t) * (1-eta_b_disc)/eta_b_disc;

* Constraints for model with NON-LINEAR LOSSES
eq_BATTERY_LOSSES_CHAR_NONLINEAR(trh(t))..
    v_p_loss_char(t) =E= 10**3 * (R + K/(1.1 - v_soc(t))) *
sqr(v_p_b_char(t)/V_r);

eq_BATTERY_LOSSES_DISC_NONLINEAR(trh(t))..
    v_p_loss_disc(t) =E= 10**3 * (R + K/v_soc(t)) *sqr(v_p_b_disc(t)/V_r);


eq_BATTERY_MAX_CHAR(trh(t))..
    v_p_b_char(t) =L= P_b_max_char*v_u_b_char(t);

eq_BATTERY_MAX_DISC(trh(t))..
    v_p_b_disc(t) =L= P_b_max_disc*v_u_b_disc(t);
```

```
eq_BATTERY_CHAR_OR_DISC(trh(t))..
    v_u_b_char(t) + v_u_b_disc(t) =L= 1;


* Diesel generator:
eq_DIESEL_MAX_GEN(trh(t))..
    v_p_d(t) =L= P_d_max * v_u_d(t);

* Solar panel:
eq_PV_CURT(trh(t))..
    PV(t) =E= v_p_pv(t) + v_p_curt(t);


MODEL MICROGRID_LINEARLOSSES /
eq_OF
eq_ENERGY_BALANCE
eq_SOC
eq_BATTERY_DYNAMICS
eq_BATTERY_LOSSES_CHAR_LINEAR
eq_BATTERY_LOSSES_DISC_LINEAR
eq_BATTERY_MAX_CHAR
eq_BATTERY_MAX_DISC
eq_BATTERY_CHAR_OR_DISC
eq_DIESEL_MAX_GEN
eq_PV_CURT
/
;

MODEL MICROGRID_NONLINEARLOSSES /
eq_OF
eq_ENERGY_BALANCE
eq_SOC
eq_BATTERY_DYNAMICS
eq_BATTERY_LOSSES_CHAR_NONLINEAR
eq_BATTERY_LOSSES_DISC_NONLINEAR
eq_BATTERY_MAX_CHAR
eq_BATTERY_MAX_DISC
eq_BATTERY_CHAR_OR_DISC
eq_DIESEL_MAX_GEN
eq_PV_CURT
/
;


*Rolling horizon implementation:
it = ceil[((SH - PH) / CH) + 1];
scalar i;


* Option file
MICROGRID_NONLINEARLOSSES.optfile=1;
```

```
for (i = 1 to it,

    t_ini = CH*(i - 1)+1;
    t_fin = t_ini + PH -1;

    trh(t) = yes$[t.ord >=t_ini and t.ord <=t_fin];

*    SOLVE MICROGRID_LINEARLOSSES MINIMIZING v_ofv USING MIQCP;

    SOLVE MICROGRID_NONLINEARLOSSES MINIMIZING v_ofv USING MINLP;

    E_b_0 = sum(t$(t.ord = t_ini + CH -1), v_e_b.l(t));

);

v_ofv_RH = SUM[t,c*v_u_d.l(t) + b*v_p_d.l(t) + a*sqr(v_p_d.l(t)) +
c_nse*v_p_ns.l(t)] * DT;

execute_unloaddi 'microgrid_results.gdx',

PV
D
v_p_ns
v_p_pv
v_p_curt
v_p_d
v_p_b_char
v_p_b_disc
v_p_loss_char
v_p_loss_disc
v_soc
v_u_d
v_ofv_RH
;

execute '=gdx2xls microgrid_results.gdx';
executeTool 'win32.shellExecute microgrid_results.xlsx';
```

# APPENDIX II. ADDITIONAL GRAPHS

The following graphs are part of the comparative analysis of energy management between optimization approaches (Chapter 6). They have been included in this appendix for the convenience of readers interested in the further examination of results obtained. To facilitate the location of specific graphs, they have been divided into two sections depending on the dataset used.

## *II.1 168-HOURS SUMMER*

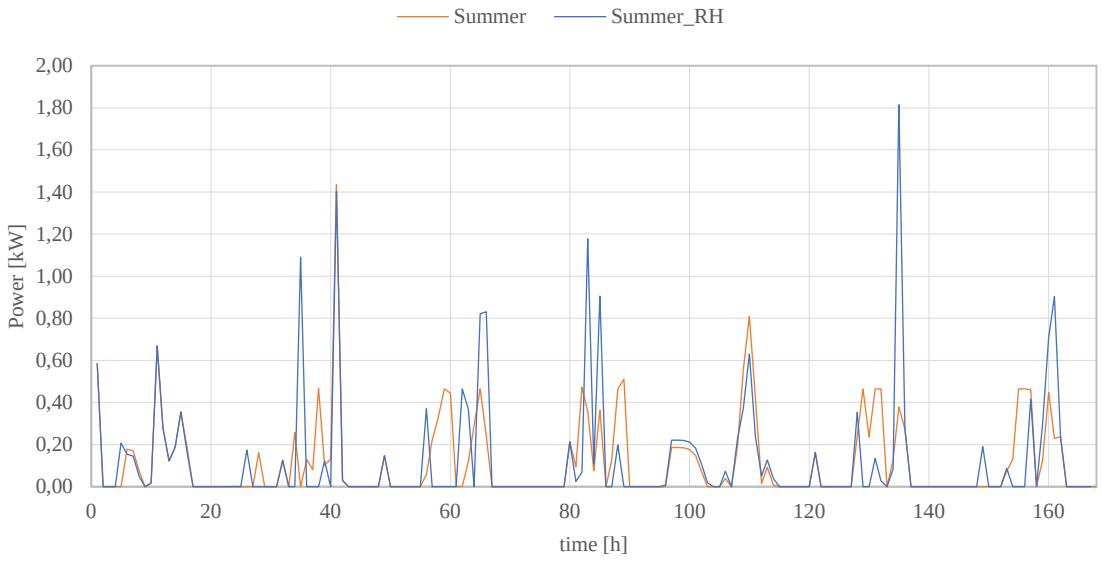


*Figure II.1: Obtained results (Bat. Char., NLL-BARON, 168 hours Summer)*

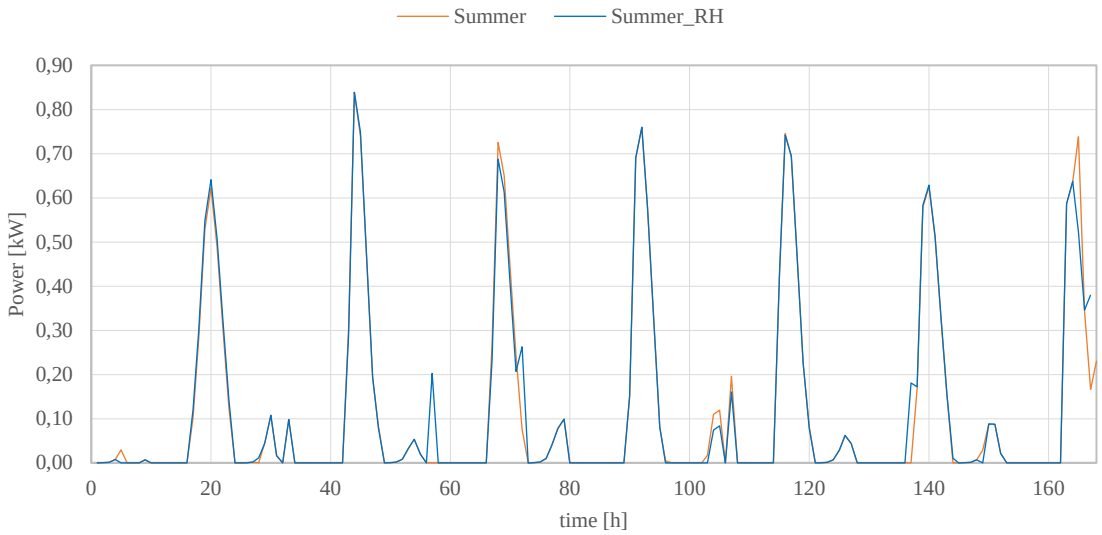


*Figure II.2: Obtained results (Bat. Disc., NLL-BARON, 168 hours Summer)*

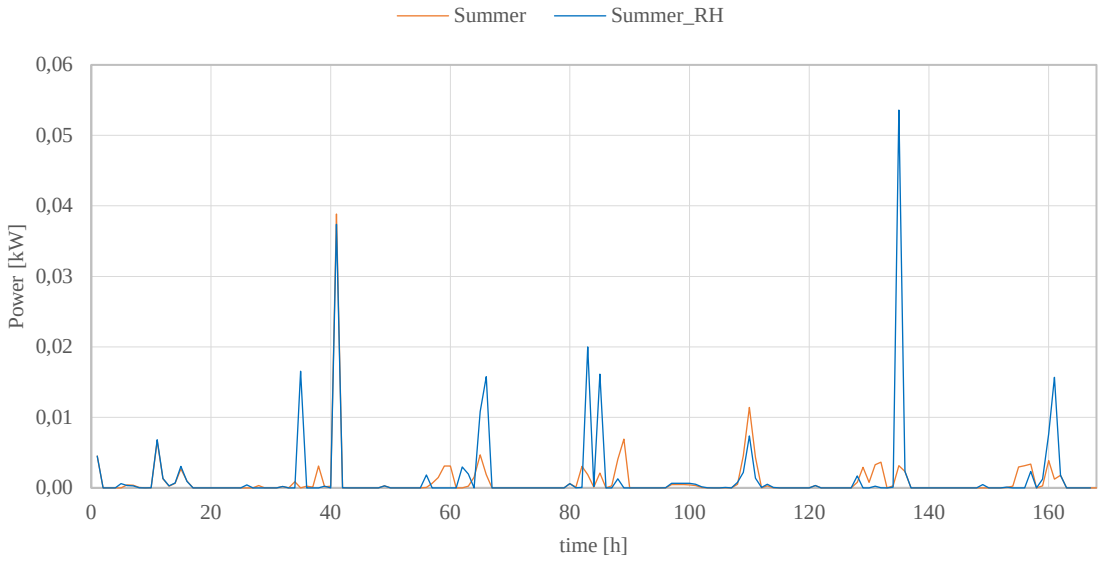


*Figure II.3: Obtained results (Losses Bat. Char., NLL-BARON, 168 hours Summer)*

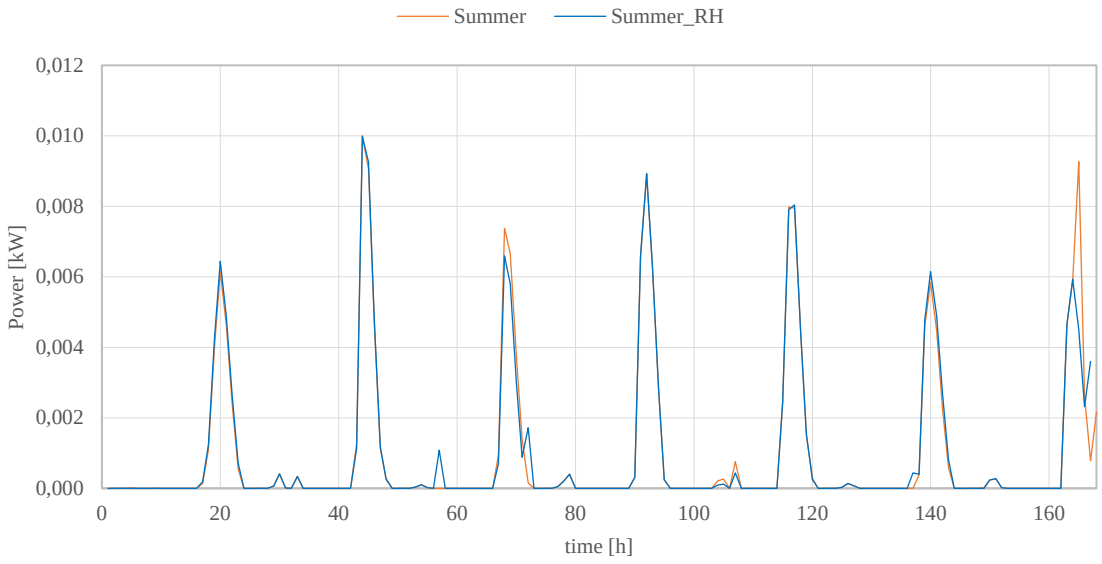


*Figure II.4: Obtained results (Losses Bat. Disc., NLL-BARON, 168 hours Summer)*

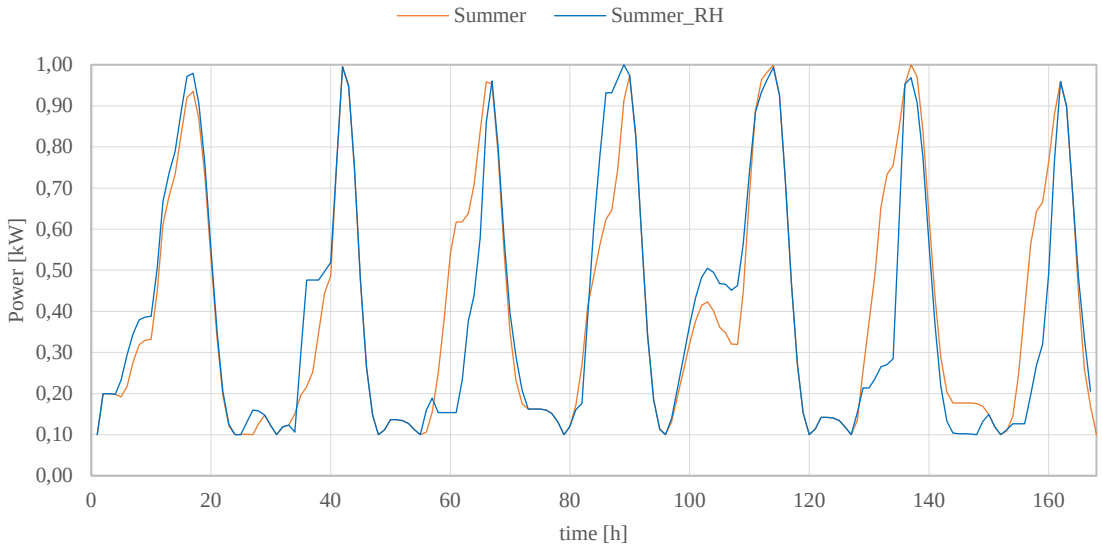


*Figure II.5: Obtained results (Losses Bat. Disc., NLL-BARON, 168 hours Summer)*

## *II.2 168-HOURS WINTER*

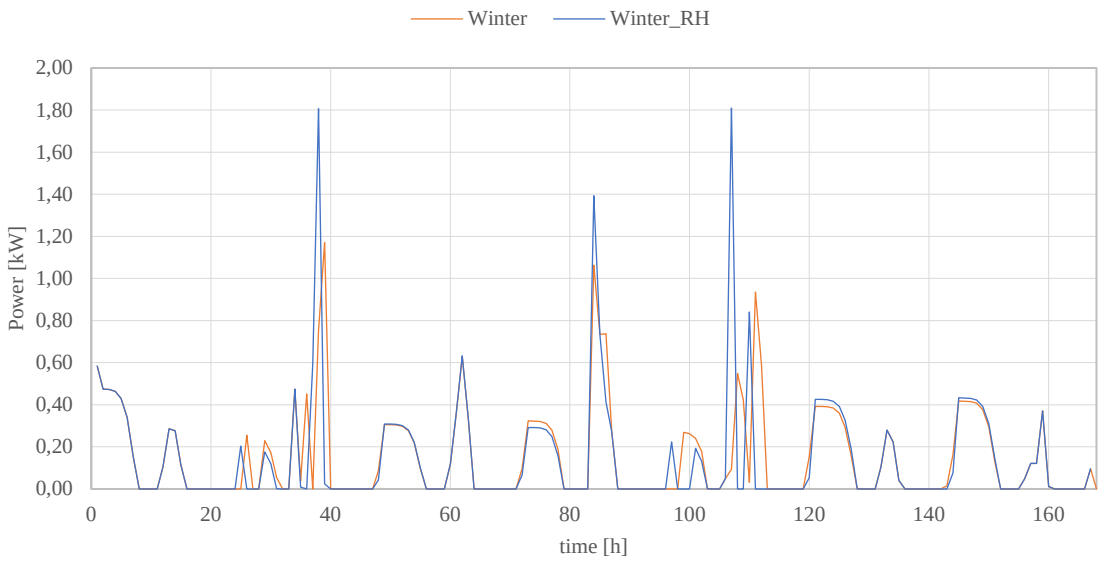


*Figure II.6: Obtained results (Bat. Char., NLL-BARON, 168 hours Winter)*

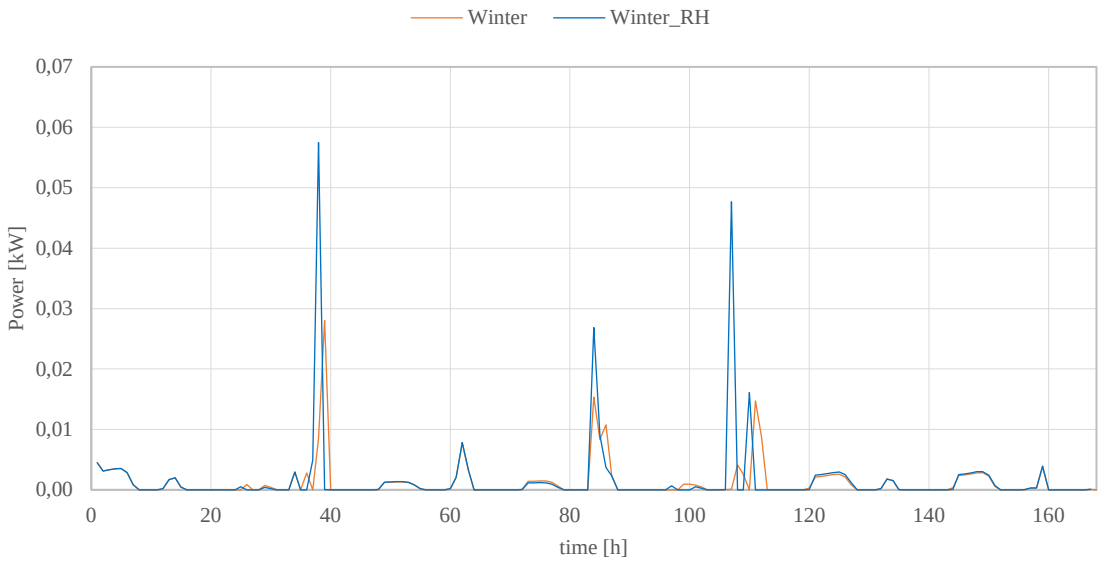


*Figure II.7: Obtained results (Losses Bat. Char., NLL-BARON, 168 hours Winter)*

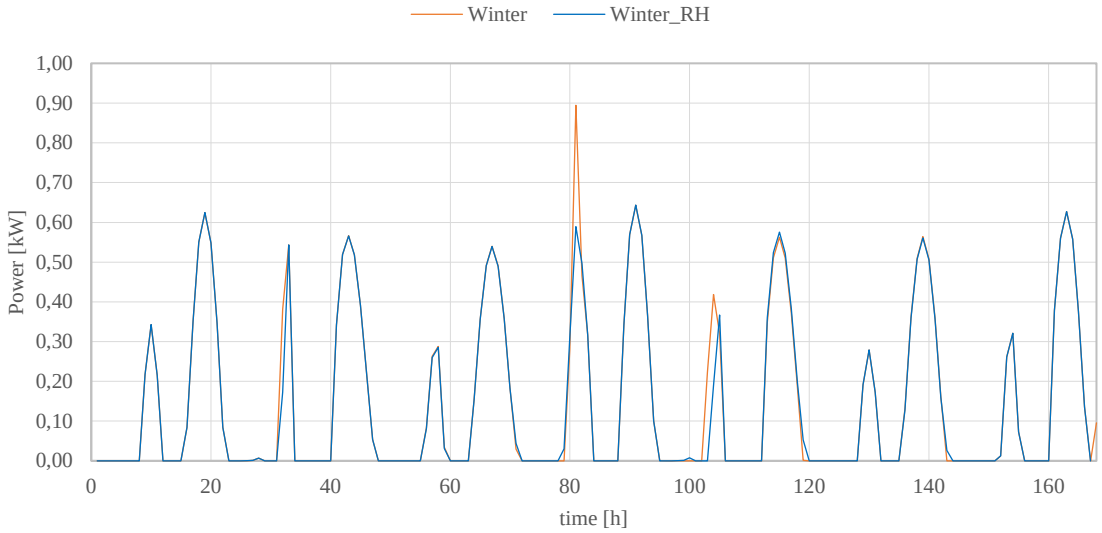


*Figure II.8: Obtained results (Losses Bat. Char., NLL-BARON, 168 hours Winter)*

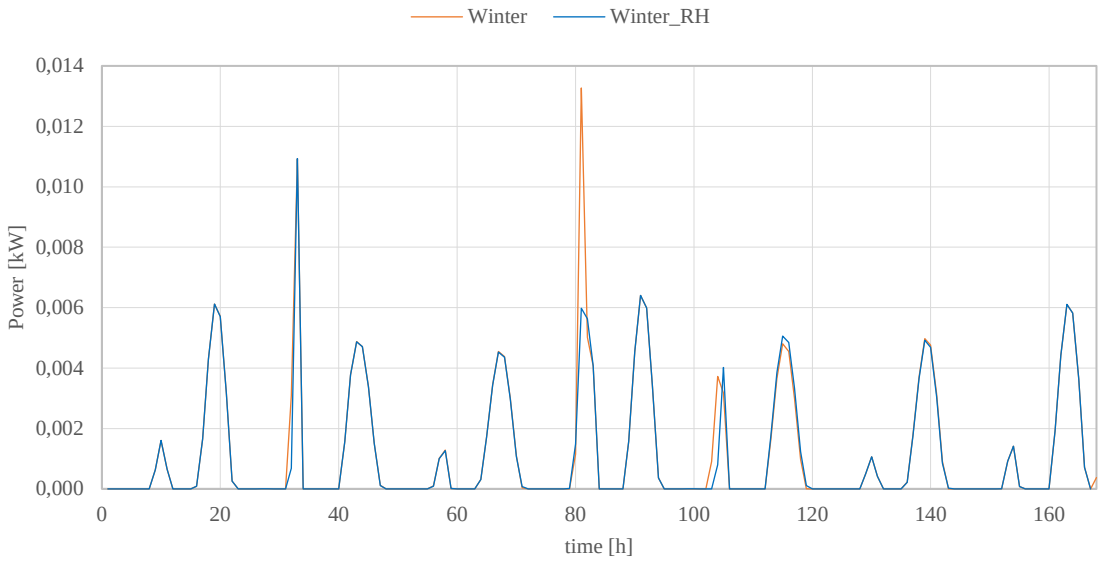


*Figure II.9: Obtained results (Losses Bat. Disc., NLL-BARON, 168 hours Winter)*

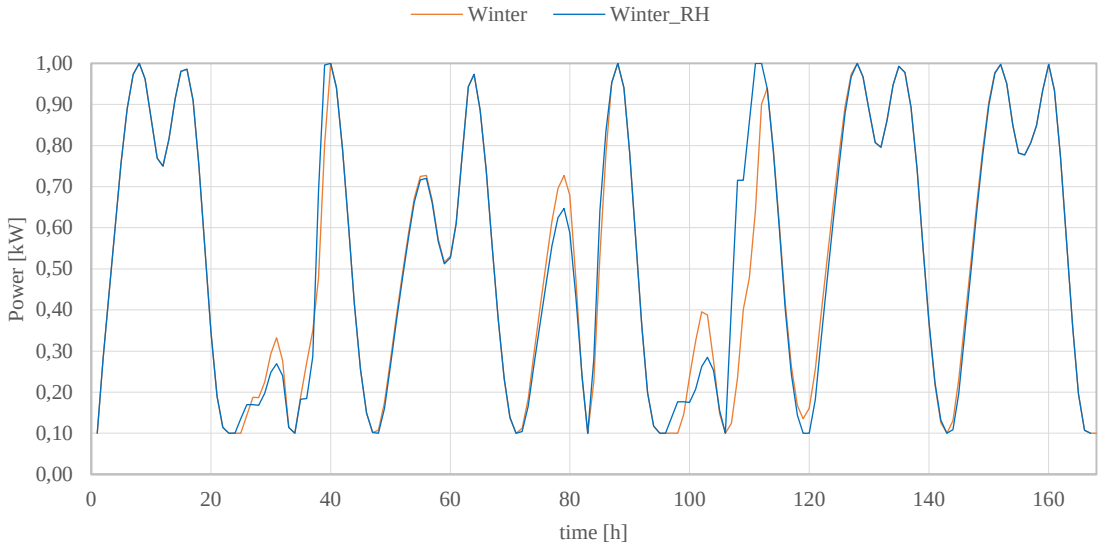


*Figure II.10: Obtained results (SoC, NLL-BARON, 168 hours Winter)*

# APPENDIX III. ALIGNMENT WITH SUSTAINABLE DEVELOPMENT GOALS

The Sustainable Development Goals (SDGs) are part of the United Nation's 2030 Agenda for Sustainable Development. These goals are aimed at building a better and more sustainable future without leaving anyone behind by addressing three core areas: economic growth, social inclusion and environmental protection. [24]


*Figure III.1: Sustainable Development Goals (Source: [24])*

This project is aligned with multiple SDGs given the importance of global commitment and involvement to accomplish them. To analyze this project's contribution to the SDGs, one primary goal and two secondary goals belonging to the remaining two core dimensions were identified.

The main goal addressed by this project is SDG 7: "Ensure access to affordable, reliable, sustainable and modern energy for all". Development of microgrid technologies is directly aimed at tackling target 7.1: "By 2030, ensure universal access to affordable, reliable and modern energy services". The improvement of energy management systems (EMS) used for microgrid operation results in a more efficient management of the connected energy sources

thereby reducing operation costs. Microgrids also increase the reliability of energy supply by providing energy from storage systems and distributed energy sources in case of a power outage. Furthermore, microgrids can provide electricity to remote communities where extending the microgrid would be too costly and, therefore, contribute to the ongoing objective of providing energy access to everyone. Sustainability is a key characteristic of microgrids since they promote the deployment of renewable energy resources, meaning this project also aligns with target 7.2: “By 2030, increase substantially the share of renewable energy in the global energy mix”.

Regarding the environmental dimension of SDGs, this project is closely linked to SDG 13: “Take urgent action to combat climate change and its impacts”, specifically target 13.2: “Integrate climate change measures into national policies, strategies and planning”. The availability of more efficient EMS will lead to a greater penetration of microgrids, hence fostering the integration of renewable energy sources (RES) in the energy mix. RES, such as solar panels and wind turbines, are clean energy sources whose operation does not produce greenhouse gases.

SDG 9 is the economic goal which is most strongly connected with this project: “Build resilient infrastructure, promote inclusive and sustainable industrialization and foster innovation”, more precisely, target 9.4: “By 2030, upgrade infrastructure and retrofit industries to make them sustainable, with increased resource-use efficiency and greater adoption of clean and environmentally sound technologies and industrial processes, with all countries taking action in accordance with their respective capabilities”. To increase the sustainability of the electric power industry, a transition towards the use of RES is necessary. This requires their deployment at both an industrial and a residential level, which can be implemented through the use microgrids. Specifically, the research and development aimed at improving energy management systems for microgrids will imply a more cost and resource efficient operation since the optimality of the decisions made regarding dispatch of energy sources and energy storage will increase.

# APPENDIX IV. BUDGET

Table IV.1 presents the budget for this project from the point of view of an independent consultant.

| Item | Unitary cost | Quantity | Total cost |
|---|---|---|---|
| Direct costs | | | |
| Consulting fees | 60.00 €/hour | 200 hours | 12,000.00 € |
| Indirect costs | | | |
| Rent and utilities | 700.00 €/month | 5 months | 3,500.00 € |
| Software license amortization | 409.29 €/month | 5 months | 2,046.46 € |
| Laptop amortization | 25.18 €/month | 5 months | 125.92 € |
| | | | **17,672.38 €** |

*Table IV.1: Budget*

The items included are described below:

- Consulting fees: Hourly rate was determined taking into account the project is carried out by a junior consultant.
- Rent and utilities: This includes office space lease, electricity, water, heating, cleaning services and internet.
- Software license amortization: The project requires a Microsoft Office 365 individual license (99 €/year) and a GAMS professional license including various modules:
    - GAMS/BASE: 3500€
    - GAMS/BARON: 3500€
    - GAMS/CONOPT: 3500€

- GAMS/DICOPT: 1750€
- GAMS/MINOS: 3500€
- GAMS/SNOPT: 3500€

The GAMS licenses will be amortized over 4 years.

- Laptop amortization: The laptop used is an HP ProBook 450 G10 with a retail price of 1,208.79€ amortized over 4 years.